The International Journal of Advanced Manufacturing Technology (2019) 105:5023–5044
https://doi.org/10.1007/s00170-019-04602-4

ORIGINAL ARTICLE

Strength properties and structure of CuCrZr alloy subjected to low-temperature KOBO extrusion and heat treatment

Paweł Ostachowski[1] · Włodzimierz Bochniak[1,2] · Marek Łagoda[2] · Stanisław Ziółkiewicz[2]

Received: 7 July 2019 / Accepted: 21 October 2019 / Published online: 18 November 2019

Abstract

KOBO extrusion of metals and alloys strongly activates the point defect generation processes, as a result of which they reach a concentration exceeding the equilibrium level by many orders of magnitude. This leads to significant acceleration of diffusion phenomena which in heat-treatable alloys may cause disturbance of the thermodynamic equilibrium between the solid solution decomposition and dissolution of precipitates. In this work, measurements of mechanical and electrical properties and structural observations Cu1Cr0.1Zr alloy subjected to low-temperature KOBO extrusion at different stages of multi-variant heat treatment were conducted. In addition, the geometry of the extruded alloy's flow zone was analyzed and the obtained results made it possible to assess the effectiveness of experimental procedures, including product formation with high extrusion ratio λ, aimed at achieving of high and thermally stable functional properties of the material.

Keywords Cu1Cr0.1Zr alloy · KOBO extrusion · Heat treatment · Mechanical properties · Electrical conductivity

1 Introduction

Age-hardenable CuCrZr alloys achieve high functional properties thanks to the application of heat or thermomechanical treatment. Due to a favorable combination of strength properties, as well as electrical and thermal parameters, the alloy can be classified as one of the so-called functional materials used for various applications, mainly in the production of high heat flux components of ITER (International Thermonuclear Experimental Reactor), but also in the manufacturing of trolley contact wire dedicated for high-speed trains on electrical railways, resistance welding electrodes, and electronic commutators [1–3].

CuCrZr alloys usually contain 0.5÷1.5 wt% Cr and 0.03÷0.3 wt% Zr; however, alloys with a chemical composition significantly exceeding the above range are also made, e.g., Cu0.3wt%Cr0.5wt%Zr [4]. "Classical" alloy contains 1.0 wt% chromium and 0.1 wt% zirconium and the remainder is copper. The solubility of chromium in copper at 1000 °C is 0.37 wt%, and so only in individual cases (for ≤ 0.37wt%Cr) will the entire chromium content pass into the copper-matrix solid solution. At 400 °C, the solubility of chromium in copper is equal to 0.03 wt% [5]. However, the data presented in paper [6] indicates that the solubility drops from the value of 0.27 wt% at 1000 °C, to below 0.02 wt% at room temperature. Paper [6] confirms that the solubility of Cr in Cu at 1000 °C is 0.27 wt% and demonstrates that it does not exceed 0.05 wt% at 500 °C.

Chromium has a special significance in the process of generating the phase structure of CuCrZr alloy. Coarse chromium particles generated during solidification, particles not dissolved during solution annealing, and chromium-rich particles precipitated during aging were identified in Cu1Cr.01Zr alloy subjected to heat treatment (supersaturation, 1000 °C/1 h, and subsequent aging, 480 °C/5 h) [7].

The fact that CuCrZr alloy owes its high strength properties due to fine, chromium-rich particles formed during aging of previously supersaturated alloy is confirmed by a series of studies. So far, the following particles have been identified: Cu_4Zr and $CrCu_2(Zr)$ [8–10]; $Cu_{51}Zr_{14}$ [11]; Cr, Cu_5Zr, and Cu [10, 12, 13].

✉ Paweł Ostachowski
pawel.ostachowski@agh.edu.pl

[1] Faculty of Non-Ferrous Metals, Division of Structure and Mechanics of Solids, AGH – University of Science and Technology, A. Mickiewicza Av. 30, 30–059 Cracow, Poland

[2] Research Network Łukasiewicz, Metal Forming Institute, Jana Pawła II St. 14, 61–139 Poznań, Poland

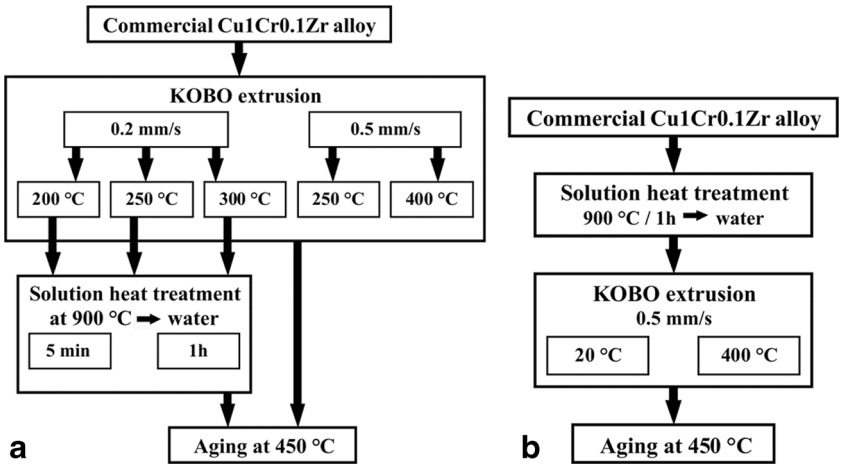

Fig. 1 Diagram of test procedure applied for KOBO extrusion of Cu1Cr0.1Zr alloy in **a** commercial and **b** supersaturated temper

A dynamic progress in scientific research in recent years and the development of new manufacturing techniques opened new possibilities to attain a particularly favorable set of mechanical and electrical properties of CuCrZr alloy. This is very significant, strength properties of Cu-0.96wt%Cr-0.067wt%Zr alloy after supersaturation (930 °C/30 min) and aging (450÷950 °C/10÷600 min), i.e., Ys ≈ 280 MPa, UTS ≈ 420 MPa, HV ≈ 150 [14], are too low for many new applications. The acceptable minimum functional hardness of CuCrZr alloy of 100 HV (UTS at room temperature above 300 MPa) makes it possible to achieve "optimum thermal conductivity," which the alloy acquires as a result of aging with hot isostatic pressing at temperatures as high as 550 °C [15]. In contrast, an alloy intended for contact wires should have the following parameters: UTS greater than 530 MPa, electrical conductivity of 78% IACS (International Annealed Copper Standard), and good thermal stability [4].

Maintaining the satisfactory strength properties of CuCrZr alloy is not easy at elevated temperature. UTS determined at room temperature, amounting to 550 MPa (YS close to 450 MPa), usually falls systematically to a level below 300 MPa at 500 °C [16] as temperature increases, which is often one of the more serious obstacles to a broader application of CuCrZr alloy in industrial practice. This adverse effect occurs regardless of the level to which CuCrZr alloy is hardened. In a tensile test at room temperature in an alloy with nominal composition (Cu1Cr0.1Zr) YS = 250 MPa, UTS = 370 MPa, and E = 40%, and at 450 °C, these parameters drop to the value of YS = 140 MPa, UTS = 190 MPa, and E = 37% [7]. In this context, Cu-0.85wt%Cr-0.09wt%Zr alloy after annealing at 970÷1000 °C/0.5÷1 h and aging at 350÷650 °C/1÷180 min particularly stands out, because at room temperature, its YS ≈ 340 MPa and UTS ≈ 445 MPa, and what is more, it is not too sensitive to overaging; therefore, its strength and plastic properties are only slightly reduced at 650 °C [17].

It is currently believed that the improvement of CuCrZr alloy's strength and electrical properties can be achieved by "refining the structure" to the form of nanoscale coherent dispersoids binding alloying atoms, as well as nanoscale grains and twins. Hardening through high dislocation densities is not possible in aged alloy due to its recovery and recrystallization [18]. However, the alloy matrix consists of copper and the alloying agents dissolve therein, which is typical at greater contents of alloying agents. As it additionally undergoes deformation and heat treatment, total strength will be mainly the result of dispersion hardening, but also depends on grain size hardening and solution strengthening. Unfortunately, these factors significantly reduce electrical conductivity, since peak-aging is associated with enormous distortion of the crystalline lattice, and leads to increased electrical resistance as electrons are strongly scattered [19].

There is a series of severe plastic deformation (SPD) methods leading to evolution of metallic materials' structure in the direction of refinement, particularly grain refinement

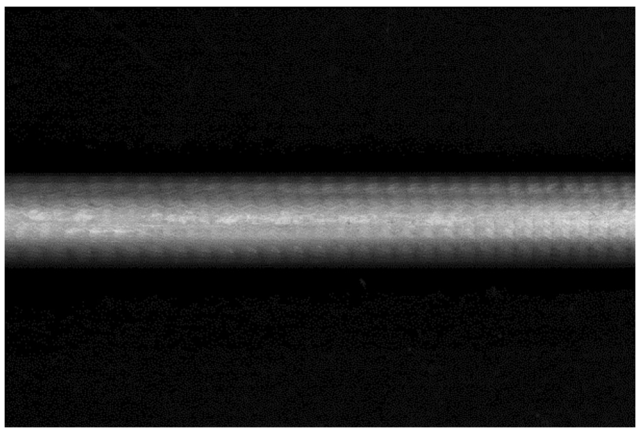

Fig. 2 Appearance of Ø12 mm extruded using the KOBO methods at a rate of 0.2 mm/s and the temperature of 250 °C

Table 1 Vickers hardness and specific electrical conductivity of CuCrZr alloy in initial temper and after KOBO extrusion at a temperature 200, 250, and 300 °C

	Billet	KOBO 200 (°C)	KOBO 250 (°C)	KOBO 300 (°C)
Hardness HV1	143.2	123.4	151.6	125.6
Conductivity σ (mS/m)	46.15	42.91	43.12	38.83

even down to the nanometric scale [20–24]. The most popular SPD method, often used during deformation of CuCrZr alloy, is the Equal Channel Angular Process (ECAP). It makes it possible to drastically increase the strength properties of Cu-0.87wt%Cr-0.06wt%Zr alloy to the level of YS = 535 MPa [25], and Cu-0.3wt%Cr-0.5wt%Zr alloy to YS = 511 MPa [4], despite the content of alloying agents (Cr and Zr) deviating from the "classical" alloy.

Unfortunately, the ECAP method has an unfavorable effect in the form of a dramatic drop in the materials' thermal stability, particularly after very high deformations, for which the phenomena of recovery and recrystallization are responsible [26, 27]. However, in Cu-0.44wt%Cr-0.2wt%Zr alloy (1040 °C/30 min + ECAP + 375 °C/15 h), precipitations strengthened the ultra-fine grain structure, and strength parameters determined at room temperature, i.e., YS ≈ 650 MPa, UTS ≈ 700 MPa, HV = 220÷225 are preserved to a significant extent up to 500 °C [23]. Significantly, the application of ECAP changes the monotonic course of CuCrZr alloy's tensile curve after supersaturation and aging, to unstable plastic flow caused by the localization of deformation in large-scale shear bands. Ultrafine grain materials have "a higher interfacial energy, higher long-range strain fields and a larger free volume than the common relaxed grain boundaries (GBs) in the pre-deformed state" [13]. The authors believe that non-equilibrium GBs were formed by way of lattice dislocation absorption by cell boundaries.

SPD methods are most commonly applied immediately prior to the aging process [23, 25, 28]. In this manner, the properties of Cu-0.45wt%Cr-0.12wt%Zr alloy (1000 °C/2 h + 8 passes of ECAP + aging 460 °C/1 h) were successfully increased to a level of approx. 700 MPa, with electrical conductivity equal to 77% IACS, as presented in paper [29]. On the other hand, however, as a result of annealing at 920 °C, followed by cold rolling (60%) and, finally, aging at 470 °C for 4 h Cu-0.3wt%Cr-0.1wt%Zr-0.05wt%Mg alloy reaches an equally high hardness (165 HV) and good conductivity (79.2 IACS) properties [30]. The rolling process generates dislocations, which constitute both diffusion paths for dissolved atoms and additional, privileged sites of precipitate formation during aging treatment, enhancing the hardening effect.

Attempts at continuous deformation of CuCrZr alloy were also made with the purpose of manufacturing substantial long continuous products [31], which is not possible in conventional processes. Promising results were obtained in continuous extrusion forming (CEF) tests carried out on Cu-0.16wt%Cr-0.12wt%Zr alloy after annealing (960 °C/2 h), where the hot-extruded alloy was subjected to cold drawing (75%) and aging (450 °C/2 h), which resulted in YS = 570 MPa, UTS = 590 MPa, $E = 17.2\%$ and electrical conductivity at the level of 77.6 IACS. The CEF process and the accompanying dynamic recrystallization made it possible to obtain submicron-scale grain sizes and a fine, dispersed morphology of precipitates. In turn, paper [19] point out that there might be a potential

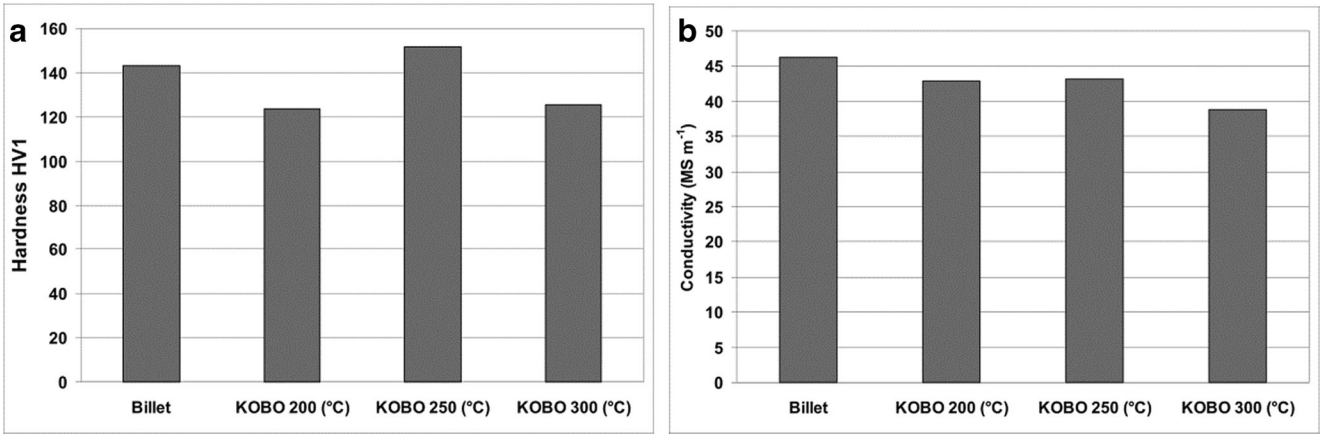

Fig. 3 Vickers hardness (**a**) and specific electrical conductivity (**b**) of CuCrZr alloy in initial temper (billet) and after KOBO extrusion at temperature of 200, 250, and 300 °C

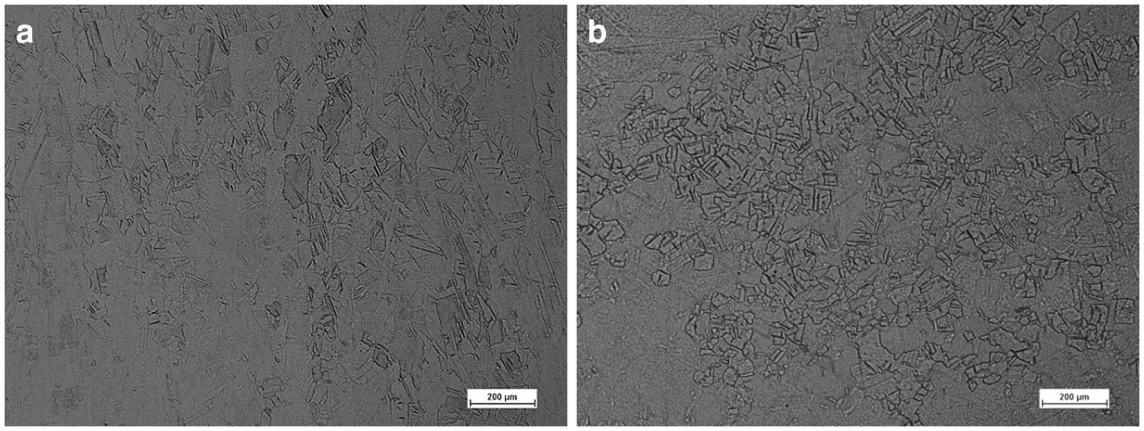

Fig. 4 Structures of Cu1Cr0.1Zr alloy in commercial temper (billet for KOBO extrusion). **a** Cross-section and **b** longitudinal section

additional alloy (Cu-1.0wt%Cr-0.1wt%Zr), in which the hardening effect is caused by nanotwins and nanograins formed during dynamic plastic deformation at liquid nitrogen temperature, which, without the involvement of the aging operation, made it possible to raise UTS to 700 MPa while maintaining high electrical conductivity (78.5% IACS).

The phenomena taking place during cryogenic dynamic deformation are described more broadly in paper [32] based on modeling studies conducted on copper. It was determined that the strong refinement of structure occurring during this process is caused by dislocations (formation of dislocation cells/grains of 121 nm), twinning (twin/matrix of 47 nm), and shear banding in the twin/matrix lamellae (nanograins of 75 nm). The higher the strain, the clearer the tendency for twinning and deformation in shear bands. Cryogenic drawing makes it possible to achieve UTS = 580 MPa and 96% IACS in pure copper [19, 33]. Even more favorable strength parameters of copper are documented in paper [34], where the high density of twins generated in the dynamic plastic deformation process at liquid nitrogen temperature resulted in the achievement of UTS equal to 610 MPa, with preservation of 96% IACS.

Due to the multitude of potential variants of heat and thermomechanical treatment of CuCrZr alloy, in many studies, strength properties are determined solely on the basis of HV hardness tests, and although these tests simplify and accelerate measurements, they also narrow their functional assessment at the same time. On the other hand, however, as shown in work [17], focused on determining the influence of aging effect on the properties of Cu-0.85wt%Cr-0.09wt%Zr alloy, there are linear relationships between HB (Brinell) hardness and YS and UTS, as shown below:

$$\mathrm{YS} = 2.0731\mathrm{HB} = 40.656 \quad \left(R^2 = 0.9745\right),$$
$$\mathrm{UTS} = 1.9313\mathrm{HB} = 166.22 \quad \left(R^2 = 0.9702\right).$$

Correct results are also obtained by applying the empirical relationship previously determined for steel to CuCrZr alloy [15]:

$$\text{for HV} \le 136,\ \mathrm{UTS} = \mathrm{HV} \cdot 3.136 + 29.4\ \mathrm{MPa}, \quad (1)$$
$$\text{for } 136 \le \mathrm{HV} \le 350,\quad \mathrm{UTS} = \mathrm{HV} \cdot 3.352\ \mathrm{MPa}. \quad (2)$$

Attempts have recently been undertaken to deform the Cu-0.81wt%Cr-0.12wt%Zr alloy using the KOBO method [35, 36]—a new version of SPD processes, based on extrusion with simultaneous, periodic, two-directional torsion [37, 38]. As shown in studies [39–41], the point defects generated during the process in large numbers reach a concentration, exceeding the equilibrium level by many orders of magnitude, which drastically increases the diffusion coefficient of the materials' ingredients and accelerates evolution of its structure. Particularly, the results presented in studies [35, 36] indicate that KOBO extrusion of supersaturated CuCrZr alloy is not only an attractive metal forming process but also an effective means of influencing the products' mechanical properties.

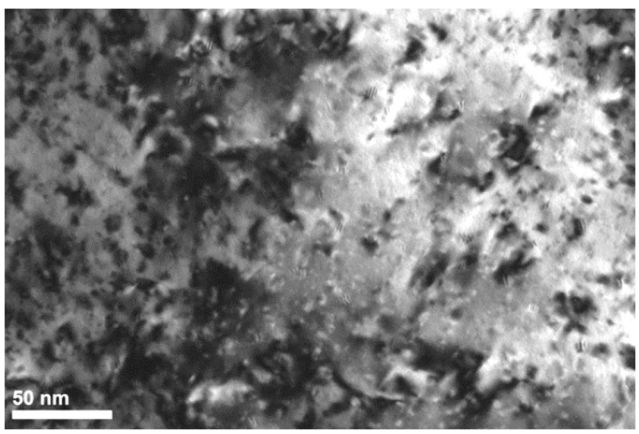

Fig. 5 Microstructure (TEM) of the sample as in Fig. 4

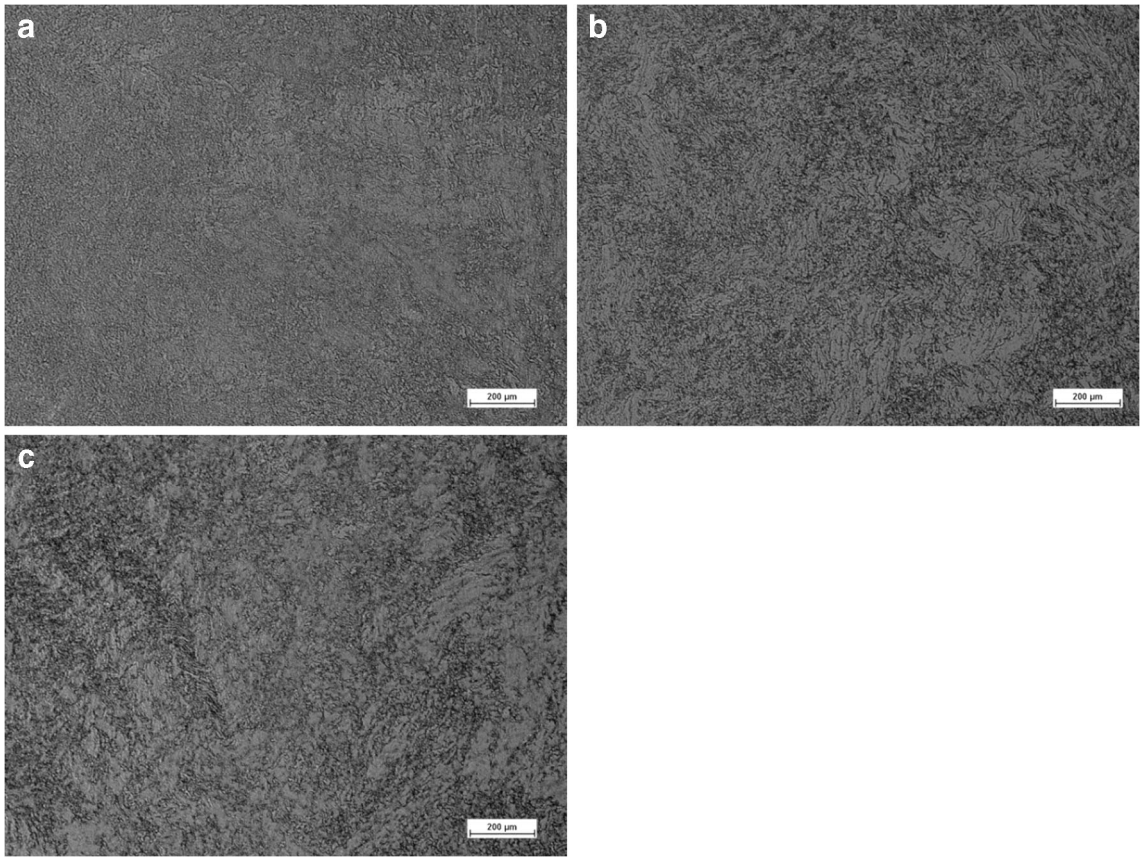

Fig. 6 Structure of cross-section of Cu1Cr0.1Zr alloy wires (Ø12 mm) extruded from commercial billet by the KOBO method with a strain rate of 0.2 mm/s, at the temperatures of **a** 200 °C, **b** 250 °C, and **c** 300 °C

In the case of dispersion-hardened alloys, depending on the parameters of the KOBO process, one of two antagonistic phenomena occur [42]:

- canceling out of the hardening effect as a result of stress relaxation around precipitates, caused by the diffusion of point defects, or
- organization of point defects into nanometric clusters (also pertains to pure metals) which additionally strengthen the alloy [40, 41].

The effect of drastic elevation of point defect concentration in CuCrZr alloy can also be achieved by neutron irradiation [43]. Strength parameters increase substantially after neutron irradiation performed at low temperatures (below 200 °C), and it is accompanied by an absence of work hardening and instability of plastic flow [16, 44]. Also, neutron irradiation of supersaturated (960 °C/3 h) and aged (460 °C/3 h) Cu-0.73wt%Cr-0.14wt%Zr alloy leads to an increase of its strength properties from YS ≈ 300 MPa and UTS ≈ 410 MPa to the level of YS ≈ 430 MPa and UTS ≈ 440 MPa, clear mechanical instability, strain softening, and, finally, localized plastic flow terminated by sample failure [44–47]. As a result of irradiation, Cu-0.49wt%Cr-0.11wt%Zr alloy supersaturated from 950 °C, cold worked 40÷45% and aged at 475÷500 °C/3 h, reaches up to YS ≈ 350 MPa and UTS ≈ 500 MPa [48].

KOBO extrusion, as well as its modified version for continuous, combined extrusion (new exrolling) [49, 50], have technological advantages and can also be used without the need for complicated tools and cumbersome procedures. The fact that the products' mechanical properties depend strictly on applied KOBO deformation parameters, mainly on the angle and frequency of the material's torsion, and are correlated with extrusion rate to a lesser extent than with process temperature and extrusion ratio λ, is significant [39].

As part of this work, measurements of mechanical (hardness and tensile tests) and electrical properties (specific electrical conductivity) and structural observations were conducted on Cu1Cr0.1Zr alloy subjected to low-temperature KOBO extrusion at different stages of multi-variant heat treatment. These studies were accompanied by the analysis of the

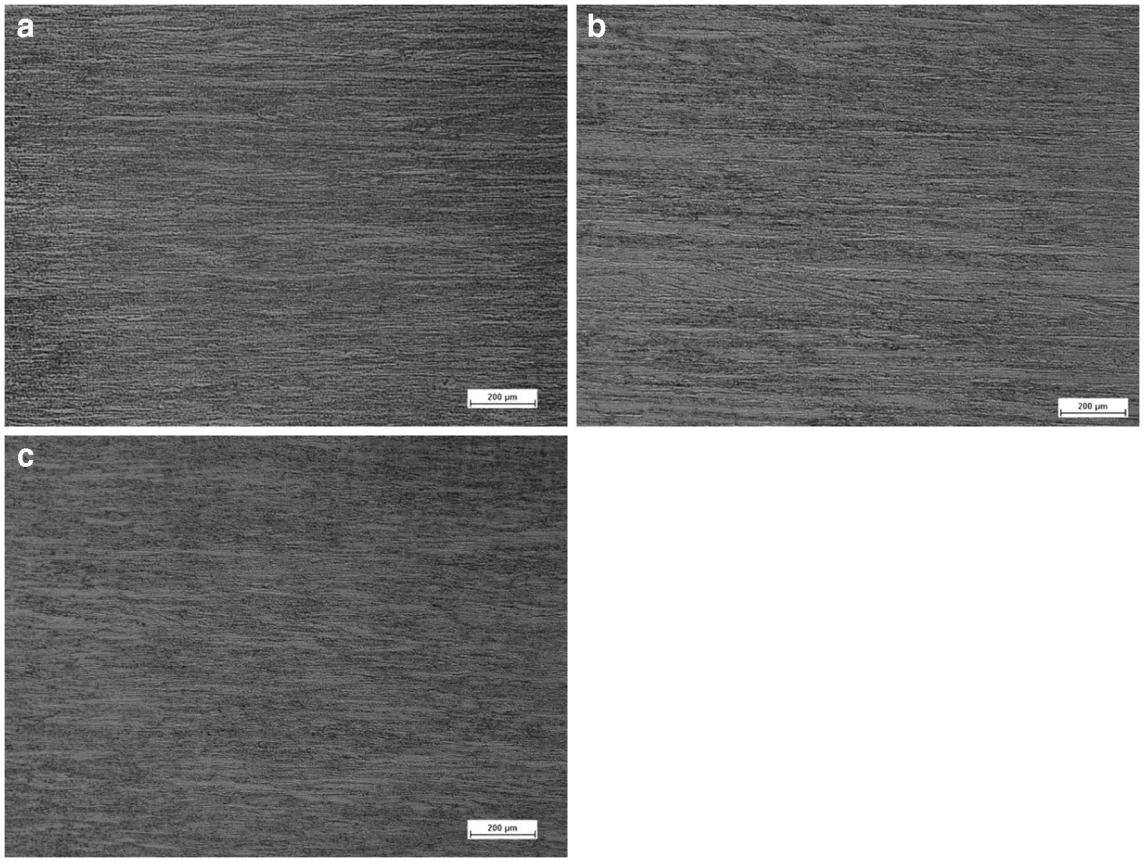

Fig. 7 Structure of longitudinal section of Cu1Cr0.1Zr alloy wires (Ø12 mm) extruded from commercial billet by the KOBO method with a strain rate of 0.2 mm/s at the temperatures of **a** 200 °C, **b** 250 °C, and **c** 300 °C

extruded alloy's flow zone's geometry, and the obtained results were used to assess the effectiveness of experimental procedures, including manufacturing with high extrusion ratio λ, aimed at achieving high, and, above all, thermally stable functional properties of the final products.

2 Procedure

The tests were conducted on commercial Cu1Cr0.1Zr alloy (in heat-treated temper), in the form of a rod with the diameter of 40 mm. The rod was cut into 40-mm-long billets and, as

Fig. 8 Typical microstructure (TEM) of Cu1Cr0.1Zr alloy wires extruded by KOBO method at 200 °C

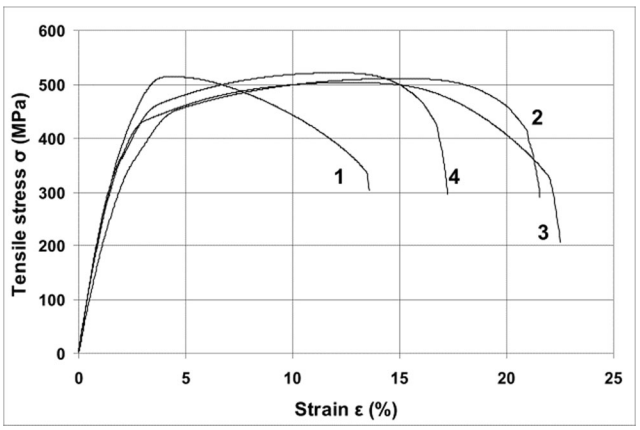

Fig. 9 Example tensile curves for CuCrZr alloy in initial temper—billet (1) and after KOBO extrusion at the rate of 0.2 mm/s at 200 °C (2), 250 °C (3), and 300 °C (4)

Table 2 Mechanical properties of CuCrZr alloy in initial temper (billet) and after KOBO extrusion at the rate of 0.2 mm/s at 200, 250, and 300 °C

	Billet	KOBO 200 (°C)	KOBO 250 (°C)	KOBO 300 (°C)
YS (MPa)	480	427	445	455
UTS (MPa)	515	504	512	522
E (%)	14.5	23.5	21.6	18.7

Table 3 Vickers hardness and specific electrical conductivity of CuCrZr alloy extruded using the KOBO method at the rate of 0.2 mm/s, and the temperatures of 200, 250, and 300 °C, and subsequently supersaturated after annealing at 950 °C for 5 min (variant I) and 1 h (variant II).

Time	5 (min)			1 (h)		
KOBO extrusion temperature (°C)	200	250	300	200	250	300
Hardness HV1	56.6	57.6	57.6	47.6	50.8	47.4
Conductivity σ (mS/m)	26.41	24.96	24.97	24.24	24.73	24.25

part of the basic experiment, extruded to a diameter of φ = 12 mm using the KOBO method at a rate of 0.2 mm/s at low temperature (200; 250 and 300 °C). Some of the products obtained in this manner were heat-treated in water from 950 °C after being held at temperature for alternatively 5 min or 1 h, and then all of them were aged at 450 °C (left part Fig. 1a), and, along with commercial alloy, used in structural observations, measurements of mechanical and electrical properties.

Tests were also conducted on commercial alloy pre-annealed at 900 °C after holding for 1 h and rapid cooling in water, followed by low-temperature KOBO extrusion preformed on fragments of the alloy (Fig. 1b) in order to check whether it is possible to preserve the alloy's capacity for aging (at 450 °C) under conditions of high concentration of point defects generated over the course of deformation. In this case, the temperature of KOBO extrusion was alternatively 20 °C (room temperature) and 400 °C. It is generally accepted that 900 °C is too low a temperature to bring about the complete dissolution of alloying agents in the copper matrix of the CuCrZr alloy. In this series of tests, in order to improve the efficiency of the process, the extrusion rate was increased from 0.2 to 0.5 mm/s, with other strain parameters left unchanged. In comparison, KOBO extrusions (rate 0.5 mm/s) of commercial CuCrZr alloy (without supersaturation) were performed at the temperatures of 250 °C and 400 °C, and subsequently aged at 450 °C (right side Fig. 1a).

Typical thermo-mechanical treatment of CuCrZr alloy is based on its supersaturation, followed by plastic deformation, and, finally, aging. Plastic deformation of the alloy in supersaturated state requires much less energy than dispersion-

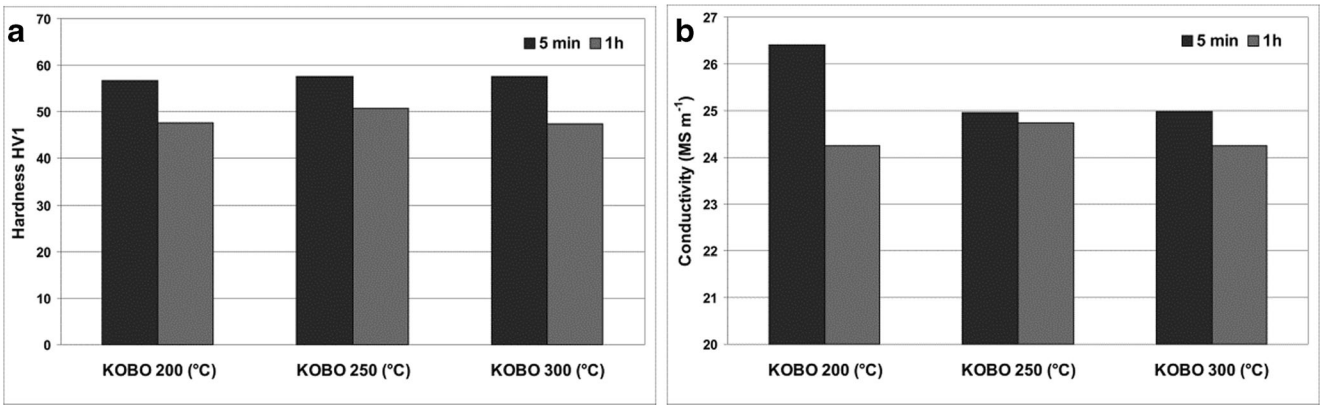

Fig. 10 Vickers hardness (**a**) and specific electrical conductivity (**b**) of CuCrZr alloy extruded using the KOBO method at the rate of 0.2 mm/s, temperatures of 200, 250, and 300 °C, and subsequently supersaturated after annealing at 950 °C for 5 min (variant I) and 1 h (variant II)

Table 4 Vickers hardness and specific electrical conductivity of CuCrZr alloy extruded using the KOBO method at the rate of 0.2 mm/s and the temperature of 200 °C, with and without supersaturation at 950 °C for 5 min or 1 h, and subsequently aged at 450 °C

	KOBO temperature (°C)	200				
	Aging time (h)	1	2	4	8	12
Without supersaturation	Hardness HV1	127.4	131.4	127.2	127	127.1
	Conductivity σ (mS/m)	45.11	47.51	49.14	49.77	49.78
After supersaturation	Hardness HV1	95	107.7	109	120.2	120
950 (°C)/5 (min)	Conductivity σ (mS/m)	40.64	46.36	46.79	46.92	47.02
After supersaturation	Hardness HV1	71.4	95.4	103.4	115	119.8
950 (°C)/1 (h)	Conductivity σ (mS/m)	34.58	43.77	45.98	47.14	47.2

Table 5 Vickers hardness and specific electrical conductivity of CuCrZr alloy extruded using the KOBO method at the rate of 0.2 mm/s and the temperature of 250 °C, with and without supersaturation at 950 °C for 5 min or 1 h, and subsequently aged at 450 °C

	KOBO temperature (°C)	250				
	Aging time (h)	1	2	4	8	12
Without supersaturation	Hardness HV1	148.2	152.2	150.4	147.8	148
	Conductivity σ (mS/m)	47.84	46.87	48.27	48.91	49.01
After supersaturation	Hardness HV1	100.3	104.7	124.0	151.2	149.6
950 (°C)/5 (min)	Conductivity σ (mS/m)	43.85	45.88	46.13	47.82	47.87
After supersaturation	Hardness HV1	80.6	90.2	107	124.8	150.2
950 (°C)/1 (h)	Conductivity σ (mS/m)	39.47	40.27	46.12	47.62	47.77

hardened alloy, where this process generates an enormous number of defects in the crystalline lattice, and not only dislocations but also point defects, and—on a larger scale—shear bands. These are all privileged sites for nucleation of the second phase, and therefore have a substantial influence on the density, size, and distribution of precipitated particles.

As part of this study, the KOBO extrusion process was performed with constant extrusion force (P = constant), equal to the maximum extrusion force of the press of $P_{max.}$ = 1.0 MN, in every case. Maintaining pressing force at such a high and unchanging level while constant extrusion rate was aimed at endowing the product with high strength properties and a uniform structure, not only on the cross-section but also throughout its entire length [40, 51]. The extrusion ratio was λ = 11.1 (cross-section of stock over cross-section of product). The angle of two-way, periodic oscillations of the die was ± 8°, and the initial frequency of oscillation was equal to 5 Hz. Constant extrusion force was maintained automatically through systematic reduction of frequency down to a final value of 2 Hz.

Because the commercial alloy was in heat-treated temper, the maximum pressing force of the KOBO press (1 MN) working at room temperature turned out to be insufficient for initiating the process, i.e., causing the alloy/product to flow out of the die, so the process was conducted within higher temperature ranges. Both the billet and container of the press

Table 6 Vickers hardness and specific electrical conductivity of CuCrZr alloy extruded using the KOBO method at the rate of 0.2 mm/s and the temperature of 300 °C, with and without supersaturation at 950 °C for 5 min or 1 h, and subsequently aged at 450 °C

	KOBO temperature (°C)	300				
	Aging time (h)	1	2	4	8	12
Without supersaturation	Hardness HV1	129.0	140.6	138.2	136.4	136.6
	Conductivity σ (mS/m)	46.94	48.14	48.49	49.44	49.57
After supersaturation	Hardness HV1	101.3	104.3	110.3	140.2	144.4
950 (°C)/5 (min)	Conductivity σ (mS/m)	40.19	44.88	46.18	47.83	48.2
After supersaturation	Hardness HV1	77.4	97.6	106.4	123.4	140.2
950 (°C)/1 (h)	Conductivity σ (mS/m)	35.38	43.41	44.59	46.27	47

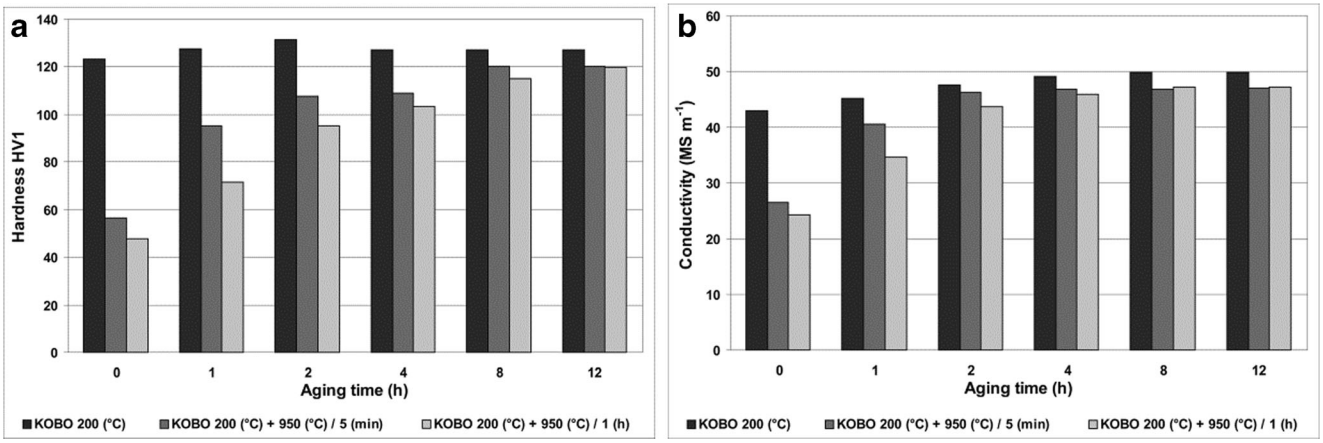

Fig. 11 Vickers hardness (**a**) and specific electrical conductivity (**b**) of CuCrZr alloy extruded using the KOBO method at rate of 0.2 mm/s, at temperature of 200 °C, with or without supersaturation at 950 °C for 5 min or 1 h, and subsequently aged at 450 °C

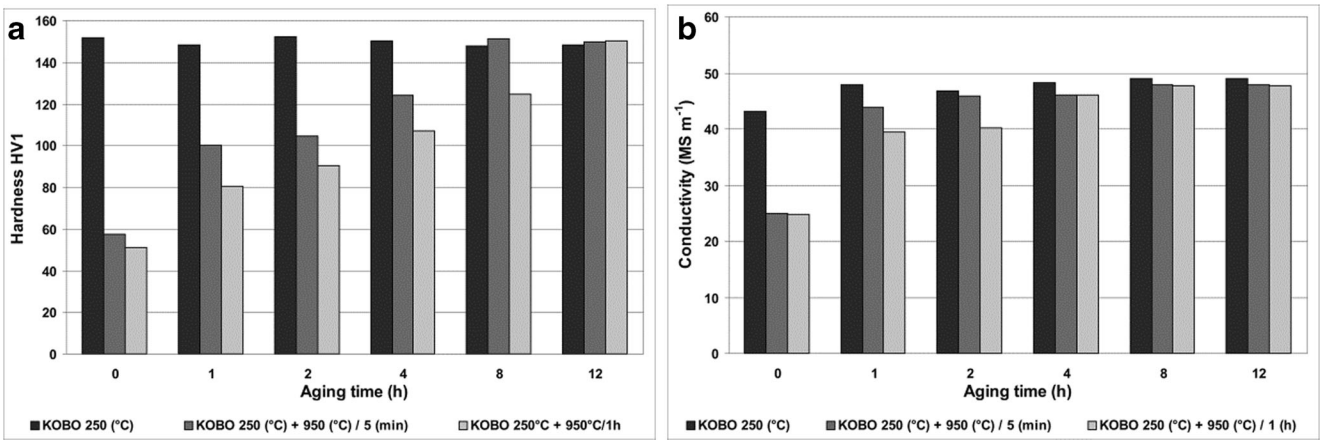

Fig. 12 Vickers hardness (**a**) and specific electrical conductivity (**b**) of CuCrZr alloy extruded using the KOBO method at the rate of 0.2 mm/s and the temperature of 250 °C, with or without supersaturation at 950 °C for 5 min or 1 h and subsequently aged at 450 °C

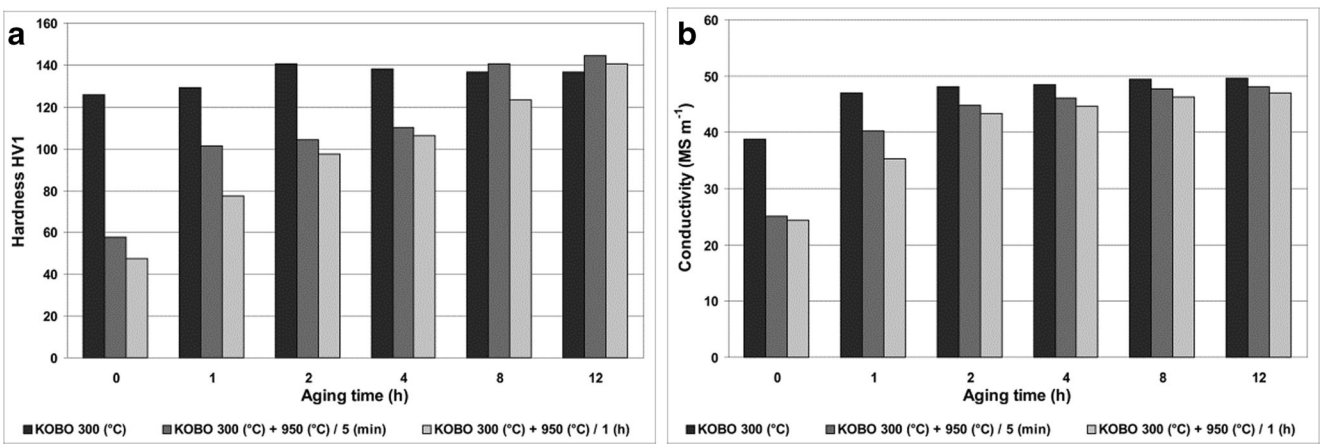

Fig. 13 Vickers hardness (**a**) and specific electrical conductivity (**b**) of CuCrZr alloy extruded using the KOBO method at the rate of 0.2 mm/s and the temperature of 300 °C, with and without supersaturation at 950 °C for 5 min or 1 h, and subsequently aged at 450 °C

were heated to these temperatures. In turn, on the output of the press, the die as well as the products were each time cooled with running water at a temperature of 20 °C.

Vickers hardness under 9.81 N load was determined for all test variants of CuCrZr alloy, and the averaged results presented in this paper were based, in every instance, on 10 unitary measurements. Tensile tests of the selected sample variants were performed at strain rate ε̇ equal to 8×10^{-3} s^{-1}. Specific electrical conductivity was measured with a Sigma Test Foerster 2.069 device, similar as in papers [52, 53] at alternating current frequency of 60 kHz, with 20 measurements taken for each of the tested materials.

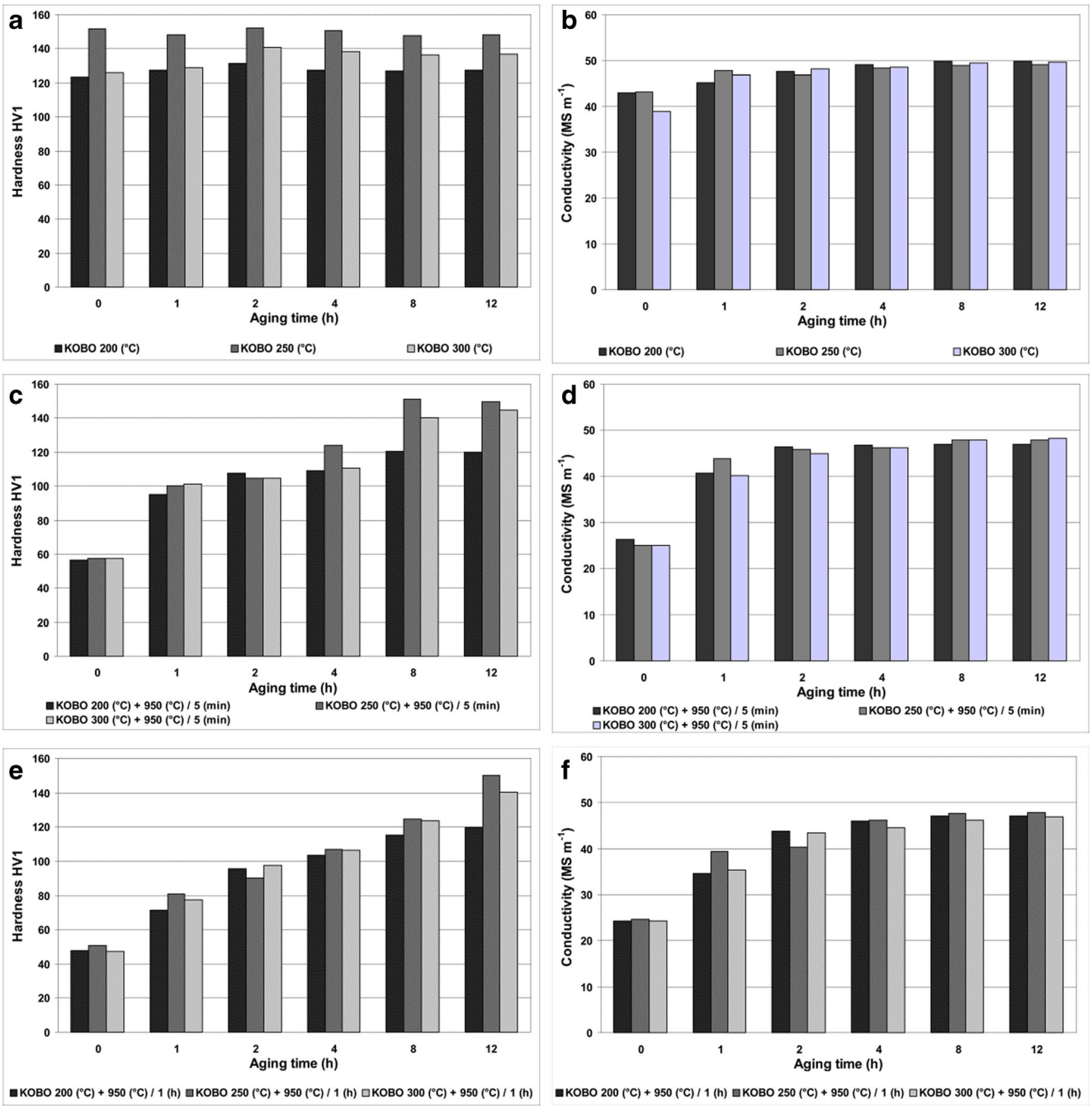

Fig. 14 Cumulative charts illustrating the influence of aging time at 450 °C on the hardness (**a**, **c**, **e**) and specific electrical conductivity (**b**, **d**, **f**) of CuCrZr alloy aged immediately after the KOBO extrusion process at strain the rate of 0.2 mm/s (**a**, **b**); after short-term (5 min) supersaturation (**c**, **d**) and after 1 h of supersaturation (**e**, **f**)

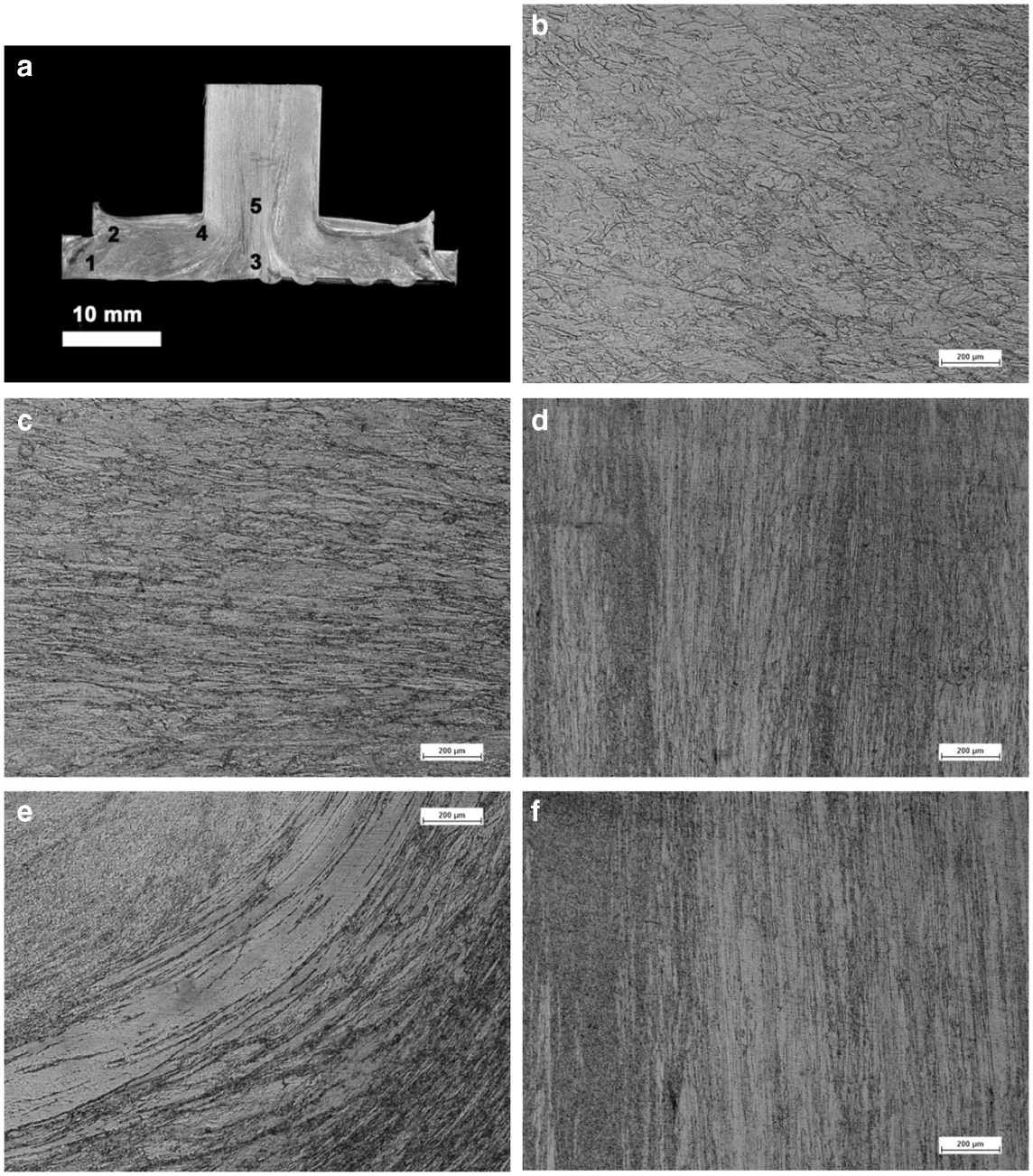

Fig. 15 Macrostructure (**a**) of shear zone in rest Cu1Cr0.1Zr alloy extruded from commercial billet by the KOBO method at the temperature of 200 °C; and microstructures of selected areas (**b**–**f**)

Based on the obtained results of mechanical properties, the relationship between HV1 and UTS was also plotted and utilized in cases where it was not possible to obtain full-size tensile samples due to the limited amount of test material (a single commercial rod of Cu1Cr0.1Zr alloy was used in the study, which guaranteed identical chemical composition, structure, and properties in all φ40 × 40 mm billet pieces made from it for testing).

Observations of structure were carried out by means of light microscopy and transmission electron microscopy. They were focused on identifying flow lines in billet-product rest areas as well as on the analysis of structural features of products, mainly the size of grains and strengthening particles. Attention was also paid to the alloy's thermal stability under overaging conditions.

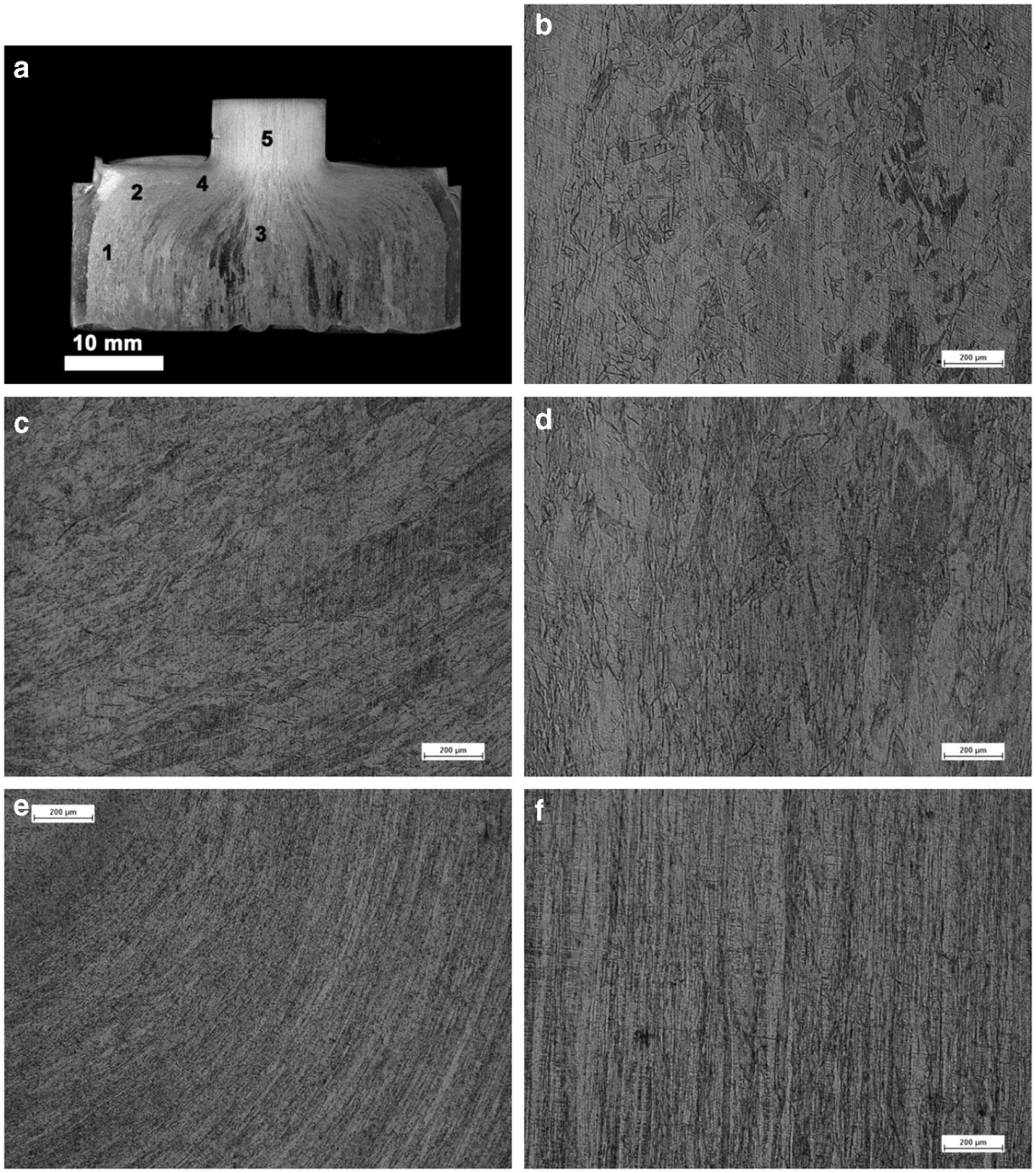

Fig. 16 Macrostructure (**a**) of shear zone in rest Cu1Cr0.1Zr alloy extruded from commercial billet by the KOBO method at the temperature of 250 °C; and microstructures of selected areas (**b**–**f**)

3 Results and analysis

The results of the first series of tests, concerning hardness, specific electrical conductivity, and initial structure of CuCrZr alloy in commercial temper and of the products in the form of Ø12-mm rods extruded from it (Fig. 2), using the KOBO method at temperature ranging from 200–300 °C, are given in Table 1 and in Figs. 3, 4, 5, 6, 7, and 8.

Regardless of the KOBO extrusion temperature, every rod was characterized by good surface quality, without discontinuities or cracks. A visible "camouflage" effect on the surface (Fig. 2) often accompanying products formed by the KOBO method is caused by the die's oscillation.

Structural observations of Cu1Cr0.1Zr alloy in commercial temper reveal its graininess ($d \approx 35$ µm), the presence of recrystallization twins, and above all, a high density of fine copper-chromium precipitates. It can be assumed that such a

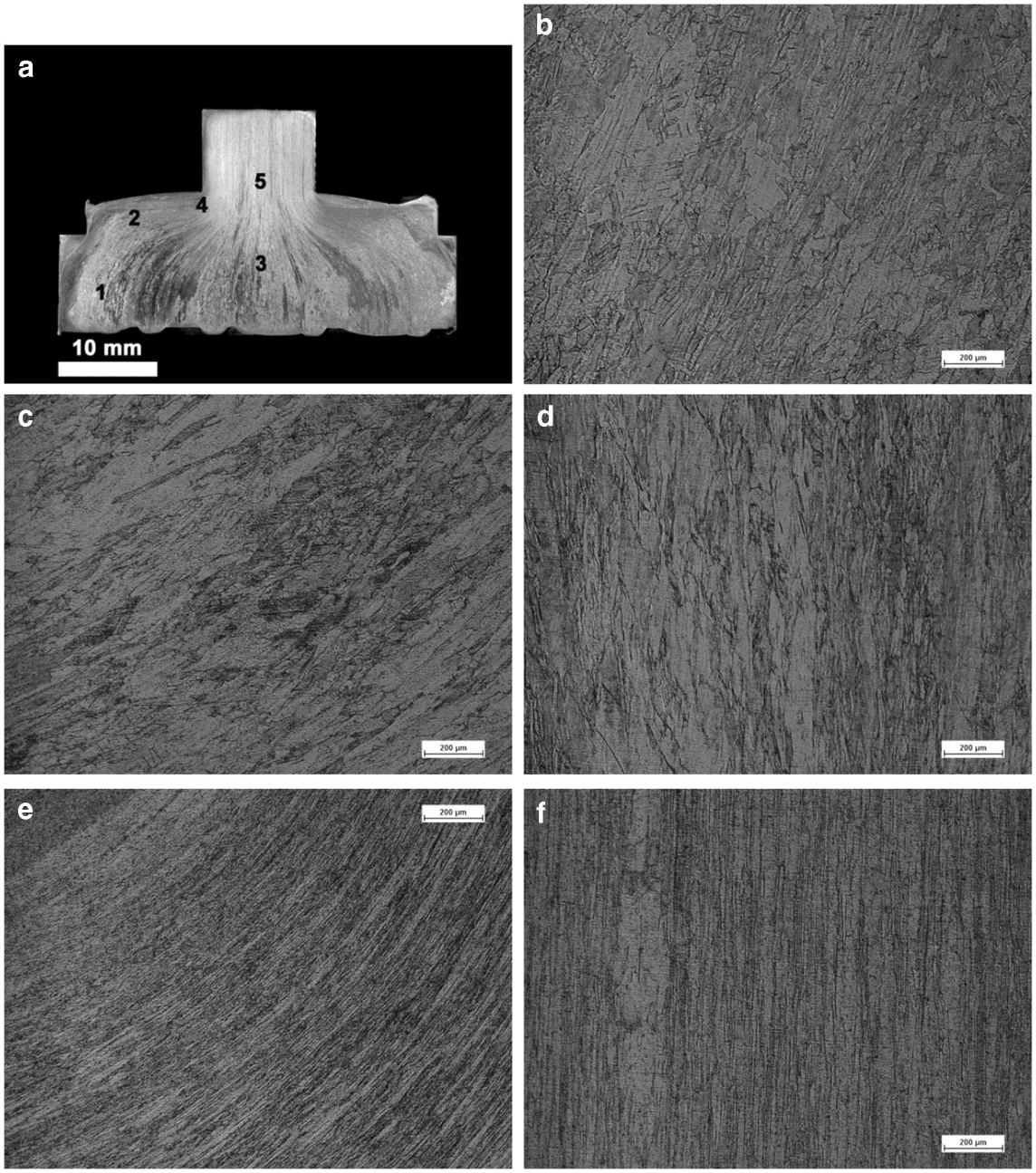

Fig. 17 Macrostructure (**a**) of shear zone in rest Cu1Cr0.1Zr alloy extruded from commercial billet by the KOBO method at the temperature of 300 °C; and microstructures of selected areas (**b**–**f**)

structure was formed as a result of the industrial heat treatment process, i.e., supersaturation (spherical grains and recrystallization twins) and aging (fine, densely distributed phase particles). TEM observations (Fig. 5) and data concerning the alloy's high hardness (143.2 HV1) bring this characterization into a clearer focus.

KOBO extrusion temperature significantly differentiates the hardness of the alloy (Fig. 3a). While products extruded at 200 and 300 °C have lower hardness (123.4 HV1 and 125.6 HV1 accordingly) than billet hardness (143.2 HV1), those extruded at 250 °C reach the value of 151.6 HV1.

Combining these data with the results of the tensile tests given in Fig. 9 and detailed in Table 2 enabled to determine the relationship between HV1 and UTS for the tested Cu1Cr0.1Zr alloy, in the form of UTS ≈ 3.59 HV1 (3), according to which the hardness of 151.6 HV1 corresponds to UTS ≈ 544 MPa. In turn (Fig. 3b), the material in the initial temper has the highest value of specific electrical conductivity (46.15 mS/m). KOBO

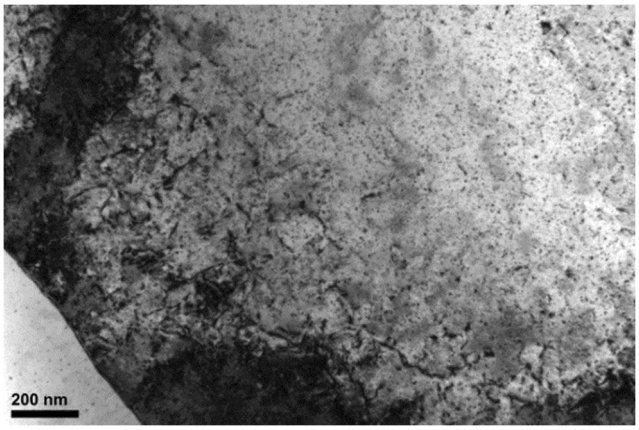

Fig. 18 Microstructure (TEM) of Cu1Cr0.1Zr alloy extruded by KOBO method with the strain rate of 0.2 mm/s at 200 °C supersaturated and aged at 450 °C for 12 h

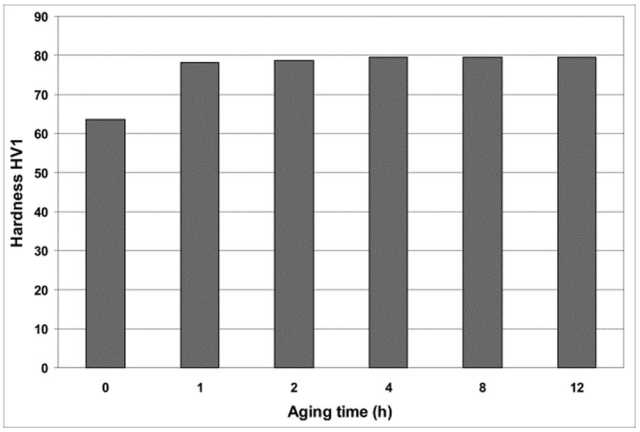

Fig. 19 Influence of aging time at 450 °C on hardness of CuCr1Zr0.1 alloy. Billet in commercial temper supersaturated at 900 °C for 1 h

extrusion causes it to decrease regardless of the applied process temperature, with the greatest drop observed for Cu1Cr0.1Zr alloy extruded at 300 °C (38.83 mS/m).

Regardless of the applied KOBO extrusion temperature, the structures of all rods bear very clear signs of plastic deformation effect. These deformations caused the fibrous structure, oriented consistently with the main direction of plastic flow (extrusion), to form. On this background, fine particles of the second phase are visible, although diverse in terms of distribution and size (Figs. 6 and 7).

According to the adopted procedure, some products manufactured in this manner were subjected to supersaturation (alternatively 950 °C/5 min—variant I; and 950 °C/1 h—variant II), as a result of which a substantial drop in the alloy's hardness was observed, to a level of approx. 57 HV1 for variant I and closed to 50 HV1 for variant II (Table 3). Similarly, as in the case of hardness, higher values of specific electrical conductivity were obtained in samples subjected to supersaturation for a shorter period of time (Fig. 10).

The effect of aging at 450 °C on the hardness and specific electrical conductivity of products obtained at different KOBO extrusion temperatures, with and without supersaturation, is shown in Tables 4, 5, and 6 and in Figs. 11, 12, and 13.

The presented data show that the level of hardness and specific electrical conductivity achieved for the other set process parameters is decided by the KOBO extrusion temperature. Aging immediately after the plastic forming process has practically no influence on hardness. Only in the case of extrusion at 300 °C was an initial increase in hardness from 125 to 140 HV1 observed over 2 h, which then stabilized at the level of approx. 137 HV1. For aging times longer than 2 h, the material may be deemed overaged (Fig. 13a). In this particular test variant (without supersaturation after extrusion—right part of Fig. 1a), an increase in specific electrical conductivity is observed for every KOBO process temperature as the time of aging at 450 °C grows.

In turn, in the KOBO extrusion with supersaturation variants (left part of Fig. 1a), a clear effect of aging time on hardness and specific electrical conductivity is observed. For example, from the perspective of the obtained set of functional properties, after supersaturation, at the most favorable extrusion temperature (250 °C), hardness increases from 57 to 150 HV1 during aging following a short-term (5 min) holding prior to supersaturation (Fig. 12a). A very similar effect is obtained when holding time until supersaturation equals 1 h, although the kinetics of this process are slower. After supersaturation, specific electrical conductivity drops to 25 mS/m, and as a result of aging, it quickly (after just 1 h) exceeds 40 mS/m and reaches almost 50 mS/m in value (Fig. 12b). The material after KOBO extrusion at 300 °C has by far the worst set of properties.

For practical reasons, attention should be paid to the variant not covering aging (without the aging operation), in which, after KOBO extrusion at 250 °C, the compact is characterized by very high strength properties, in particular, hardness reaching 151.6 HV1 (which corresponds with UTS ≈ 545 MPa) and specific electrical conductivity at the level of 43.12 mS/m.

Figure 14 presents experimental data in a manner which enables its unambiguous assessment in terms of the influence

Table 7 Influence of aging time at 450 °C on Vickers hardness of CuCrZr alloy supersaturated from the temperature of 900 °C after holding for 1 h

	Billet after supersaturation 900 (°C)/1 (h)					
Aging time (h)	0	1	2	4	8	12
HV1 hardness	63.48	78.22	78.7	79.46	79.5	79.48

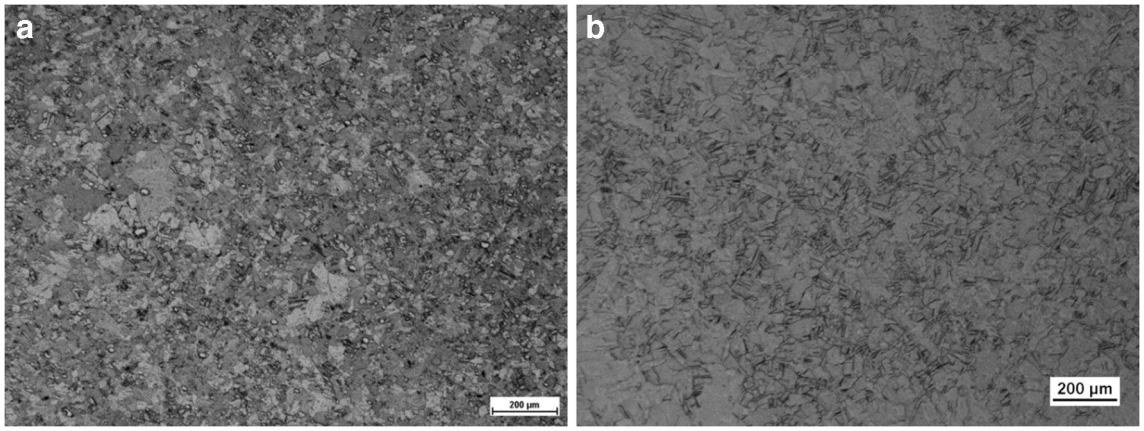

Fig. 20 Structure of Cu1Cr0.1Zr alloy supersaturated at 900 °C/1 h. **a** Cross-section. **b** Longitudinal section

of individual parameters of the KOBO process and heat treatment. It shows that the greatest hardness immediately after the extrusion process is obtained for the temperature of 250 °C which equals 151.6 HV1 (UTS ≈ 545 MPa) and exceeds the hardness of the stock material, considered to be in the state of highest hardening (143.2 HV1–UTS ≈ 515 MPa). As a result of applying heat treatment involving aging immediately after the extrusion process, the material extruded at the same temperature (250 °C) and aged at 450 °C for 2 h is characterized by the greatest hardness. However, the increase in hardness caused by aging is small (152.2 HV1). In all tested variants, aging causes specific electrical conductivity to rise both immediately after extrusion and when preceded by supersaturation, up to the level of 50 mS/m.

The obtained results indicate high hardness ~ 150 HV1 (corresponding with—according to Eq. 3—UTS ≈ 540 MPa) and good thermal stability of annealed (aged) not previously supersaturated products. In turn, the application of full heat treatment (supersaturation and aging) to commercial CuCrZr alloy extruded by means of the KOBO method makes it possible to reproduce its high hardness only after many hours of aging. Interestingly, the process responsible for hardening the alloy (particle precipitation) progresses more rapidly after 5 min of alloy annealing (supersaturation from 950 °C) than after 1 h.

In the further part of this paper, an attempt was made to answer the question whether the alloy's diverse mechanical and electrical properties are reflected (or can be revealed) in its structure. Figures 15, 16, and 17 present macrostructures of the alloy's butts after the extrusion process and microstructures of areas typical for material flow during the KOBO process.

The revealed structures contain traces of plastic flow localized in shear bands, typical for large deformations and preserved due to low extrusion temperature. It can be noted that the structure's evolution from granular (commercial alloy) to fibrous (products) has a marginal influence on the alloy's hardness, which confirms the opinion that its strength properties are determined, to the greatest extent, by much finer structure elements, most likely particles of the second phase. This is confirmed by TEM observations (Figs. 4 and 7), which indicate a very strong similarity of the alloy's microstructure before and immediately after KOBO extrusion.

Structures of commercial alloy extruded according to the KOBO method into Ø12-mm rods and subsequently heat-treated under the following conditions: supersaturation 950 °C/5 min and aging 450 °C/4 h or alternatively: supersaturation 950 °C/1 h and aging 450 °C/12 h, did not vary significantly from those observed in commercial alloy. Their characteristic feature is granularity—an effect arising from recrystallization of the alloy during supersaturation. Fine particles of the second phase, well-visible under an electron microscope, complete the picture (Fig. 18).

Table 8 Vickers hardness of CuCrZr alloy extruded by the KOBO method at the temperature of 20 °C and the rate of 0.5 mm/s, subsequently aged at the temperature of 450 °C. Billet after supersaturation at 900 °C/1 h

	Supersaturated billet, KOBO 20 (°C), extrusion rate 0.5 (mm/s)					
Aging time (h)	0	1	2	4	8	12
HV1 hardness	121.2	132.2	138.4	136	132.2	93.84

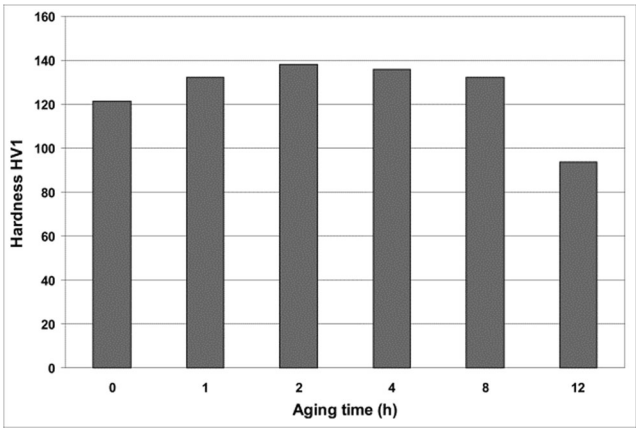

Fig. 21 Influence of aging time at 450 °C on hardness of CuCr1Zr0.1 alloy after KOBO extrusion at the rate of 0.5 mm/s and the temperature of 20 °C. Billet after supersaturation 900 °C/1 h

The data given in Table 7 and in Figs. 19 and 20 unambiguously suggest the occurrence of recrystallization of commercial alloy supersaturated (annealed) at 900 °C for 1 h. Unfortunately, satisfactory supersaturation did not take place (~ 63 HV1), as indicated by the small effect of aging and an unsatisfactory final value (80 HV1)—hardness changed by approx. 15 HV1.

A similar effect of aging (hardness change ~ 17 HV1) can be observed in the alloy previously supersaturated (900 °C/1 h) and KOBO-extruded at the rate of 0.2 mm/s (and the temperatures of 20 °C and 400 °C). However, in this case, as a result of the KOBO process performed at room temperature, the alloy's hardness reaches the value of approx. 120 HV1 (Table 8 and Fig. 21), while aging for 2 h at 450 °C raises it to the level of nearly 140 HV1 (UTS ≈ 500 MPa). It is worth noting that extending aging time leads to overaging, which manifests itself as a drop in hardness (after 12 h to ~ 95 HV1). The microstructure of the alloy after KOBO extrusion presented in Fig. 22 on longitudinal cross-sections reveals traces of low-temperature deformation in the form of clearly formed fibrous structure.

If KOBO extrusion of supersaturated (900 °C/1 h) alloy takes place at 400 °C, it hardens to a hardness of approx. 110 HV1 (Table 9, Fig. 23). Cu1Cr0.1Zr alloy reaches maximum hardness, equal to 130 HV1 (UTS ≈ 467 MPa), after 2 h of aging, and extending the time to 4, and in particular, 12 h, reduces it to a level close to 120 and 115 HV1, respectively. The temperature of 400 °C turns out to be too low for the alloy recrystallization process to occur, and just as during KOBO extrusion at room temperature, a fibrous structure of the material is dominant (Fig. 24), although in a slightly "milder" form. On the other hand, based on the alloy's documented susceptibility to heat treatment (Fig. 23), the possibility of its supersaturation in the KOBO extrusion process should be accounted for.

Data for commercial Cu1Cr0.1Zr alloy extruded (at the rate of 0.5 mm/s) using the KOBO method at 250 °C, and alternatively at 400 °C and subsequently annealed (aged at 450 °C), are given in Tables 10 and 11 and in Figs. 25 and 26. As a result of this procedure, the alloy reaches a high hardness (148.6 HV1 for extrusion temperature 250 °C and 150.4 HV1 for 400 °C), which was also observed earlier, in the case of KOBO extrusion of commercial Cu1Cr0.1Zr alloy (Fig. 12) at the rate of 0.2 mm/s. Lower extrusion temperature (250 °C) means that, during aging, the alloy's hardness drops from nearly 150 HV1 to approx. 140 HV1 and is maintained at this level for 12 h. During KOBO extrusion at 400 °C, in turn, the hardness of the alloy immediately achieves the value of close to 150 HV1 (UTS ≈ 538 MPa), which practically does not change over the 12 h of aging.

The microstructure of CuCrZr alloy in commercial temper, immediately after KOBO extrusion at 250 °C, with the

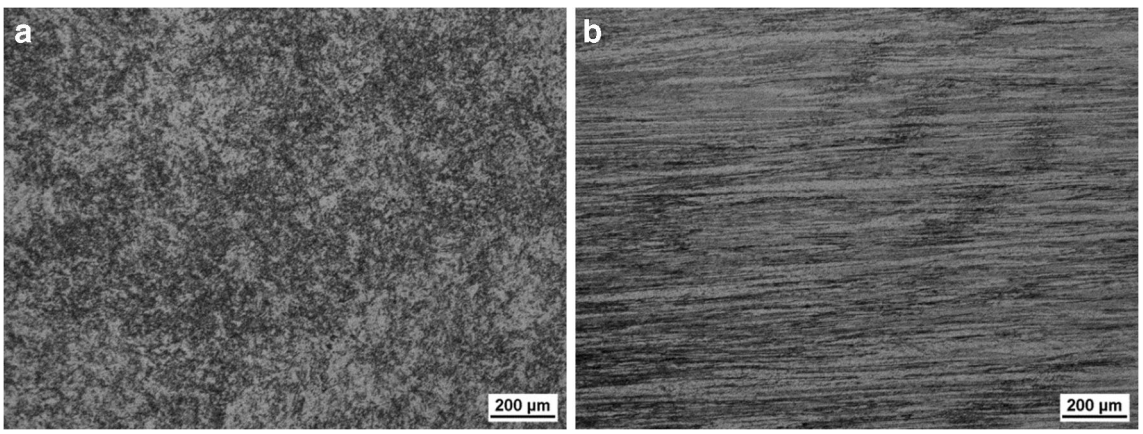

Fig. 22 Structures of Cu1Cr0.1Zr alloy (in supersaturated temper 900 °C/1 h) after KOBO extrusion at the rate of 0.5 mm/s and temperature of 20 °C. **a** Cross-section. **b** Longitudinal section

Table 9 Vickers hardness of CuCrZr alloy extruded by the KOBO method at the temperature of 400 °C and the rate of 0.5 mm/s, and subsequently aged at temperature 450 °C. Billet after supersaturation at 900 °C/1 h

	Supersaturated billet, KOBO 400 (°C), extrusion rate 0.5 (mm/s)					
Aging time (h)	0	1	2	4	8	12
HV1 hardness	107.2	110.4	130.4	124.2	119.8	116

extrusion rate of 0.5 mm/s (Fig. 27), is characterized by greater non-uniformity than in the case of the same material, but extruded 2.5 times slower (Figs. 6b and 7b). In the alloy extruded at 400 °C, clusters of large copper-chromium precipitates are observed on the background of the fibrous structure (Fig. 28). Typical for all microstructures revealed on cross-sections of the CuCrZr alloy, regardless of the extrusion variant, are traces of more or less distinct swirls in the alloy's flow lines, associated with the oscillating torsion of the alloy extruded by the KOBO method.

4 Commentary

The studies described in works [54–57] show that SPD processes not only lead to fragmentarization, particularly grain refinement, and dissolution of precipitates, but may also induce phase transformations [54]. In such case, there are questions regarding the formation [57, 58] or decomposition of a supersaturated solid solution with precipitation of the second phase [59, 60], as well as about the dissolution of precipitates [61, 62]. Diffusive phase transformations need long-range mass transfer, which is ensured by the presence of crystal defects [55, 56], particularly vacancies and interstitial atoms, which are intensively generated during SPD processes [40, 55, 63]. In this case, according to the Maxwell-Boltzmann distribution function, the diffusion coefficient $\boldsymbol{D}$ can be presented in the form of [45]:

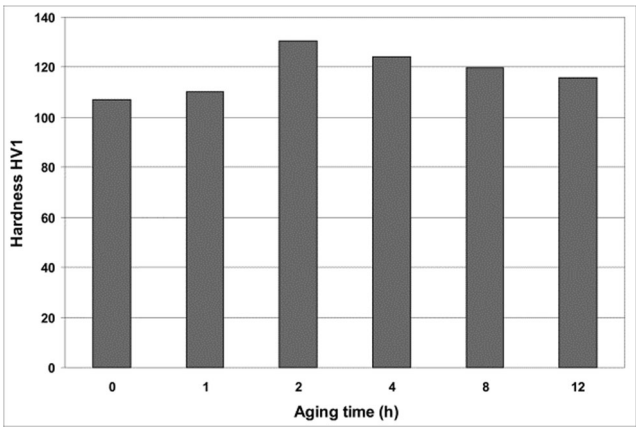

Fig. 23 Influence of aging time at 450 °C on hardness of CuCr1Zr0.1 alloy after KOBO extrusion at the rate of 0.5 mm/s and the temperature of 400 °C. Billet after supersaturation 900 °C/1 h

$$D = D_0 \cdot c_d \cdot exp\left(\frac{-E_m}{k_B \cdot T}\right) \tag{3}$$

where D_o is the geometry-frequency factor, c_d is the concentration of point defects occurring as a result of plastic deformation, E_m is the migration energy of defect, k_B is Boltzmann's constant, and T is the absolute temperature.

At 20 °C, the equilibrium concentration of vacancies in copper is very low, around 10^{-17}. The equilibrium concentration of self-interstitial atoms has a negligibly low value (lower than 10^{-34}), which is why their role in the diffusion process is generally ignored. However, tests carried out on aluminum showed [39, 41] that intense generation of vacancies and interstitial atoms occurs in the KOBO extrusion process, leading to their high concentration ($\boldsymbol{c_d} \approx 10^{-9}$), which, along with the experimentally determined [39], extraordinarily low (0.06 eV) migration energy of interstitial atoms (earlier estimated at the level of 0.06÷0.15 eV) [64–66], results in the material reaching a state that is far from equilibrium. Considering the fact that $\boldsymbol{D_o}$ for aluminum is 1.7×10^{-4} m^2/s, and the converted value of $\boldsymbol{E_m} = 9.6 \times 10^{-21}$ J, the diffusion coefficient $\boldsymbol{D}$ is equal to approx. 10^{-14} m^2/s at room temperature, and diffusion processes can occur very rapidly in materials deformed according to the KOBO method, even without heating. For comparison, it should be added that, in equilibrium (static) conditions, at room temperature, the diffusion coefficient reaches the level of just 10^{-30} m^2/s, and its value, equal to 4.2×10^{-14} m^2/s, corresponds to the temperature of 500 °C [67, 68].

Generally speaking, an overbalance of point defects' concentration disturbs the thermodynamic equilibrium [69], although in heat-treatable alloys, during SPD processes, dynamic equilibrium may occur between decomposition of the solid solution and dissolution of precipitates [55].

As shown [40, 70], pure zinc and aluminum reach high strength properties that are thermally and mechanically stable as a result of low-temperature KOBO extrusion. Their level depends on process parameters, particularly on the extrusion

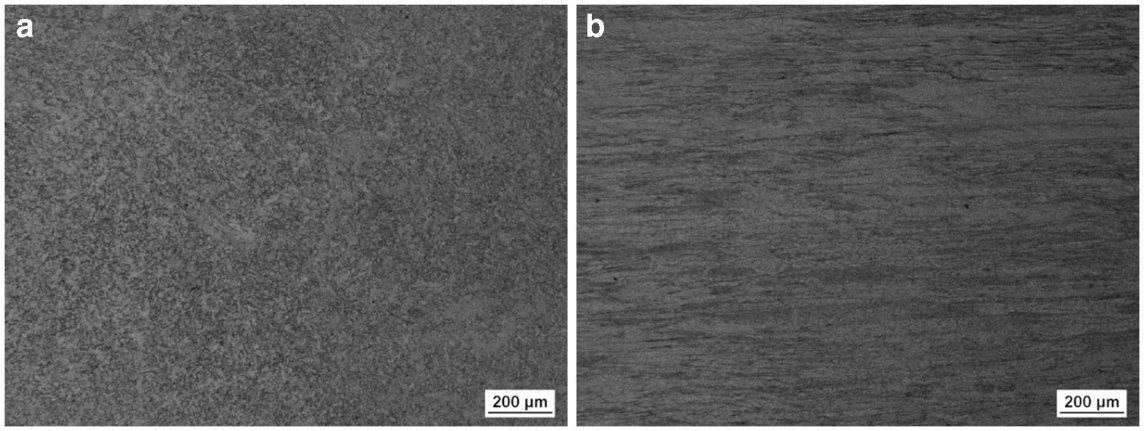

Fig. 24 Structures of Cu1Cr0.1Zr alloy (in supersaturated temper 900 °C/1 h) after KOBO extrusion at the rate of 0.5 mm/s and the temperature of 400 °C. **a** Cross-section. **b** Longitudinal section

Table 10 Vickers hardness of CuCrZr alloy extruded by the KOBO method at the temperature of 250 °C, and subsequently aged at the temperature of 450 °C. Commercial billet, extrusion rate 0.5 mm/s

	Commercial billet, KOBO 250 (°C), extrusion rate 0.5 (mm/s)					
Aging time (h)	0	1	2	4	8	12
HV1 hardness	148.6	147.6	145.2	143.4	140.8	139.6

Table 11 Vickers hardness of CuCrZr alloy extruded by the KOBO method at the temperature of 400 °C, and subsequently aged at the temperature of 450 °C. Commercial billet, extrusion rate 0.5 mm/s

	Commercial billet, KOBO 400 (°C), extrusion rate 0.5 (mm/s)					
Aging time (h)	0	1	2	4	8	12
HV1 hardness	150.4	151.8	151.6	151.4	148.8	149.6

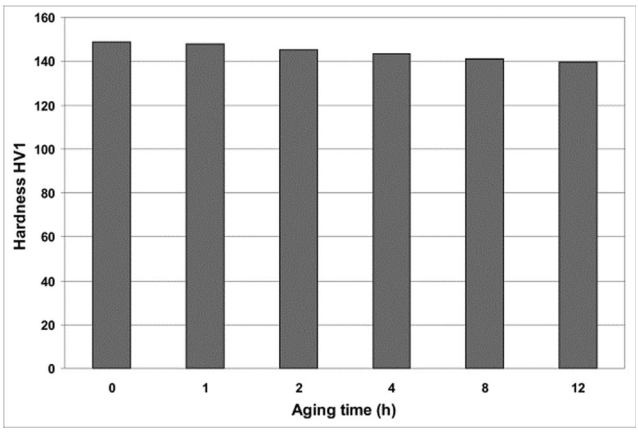

Fig. 25 Influence of aging time at 250 °C on the hardness of CuCr1Zr0.1 alloy after KOBO extrusion at 250 °C. Billet in commercial temper, extrusion rate 0.5 mm/s

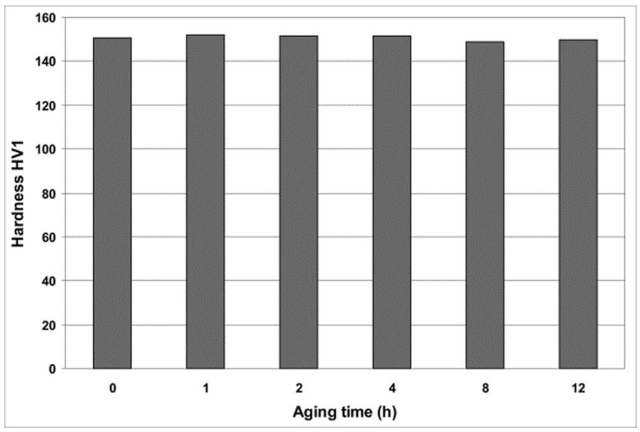

Fig. 26 Influence of aging time at 450 °C on the hardness of CuCr1Zr0.1 alloy after KOBO extrusion at 400 °C. Billet in commercial temper, extrusion rate 0.5 mm/s

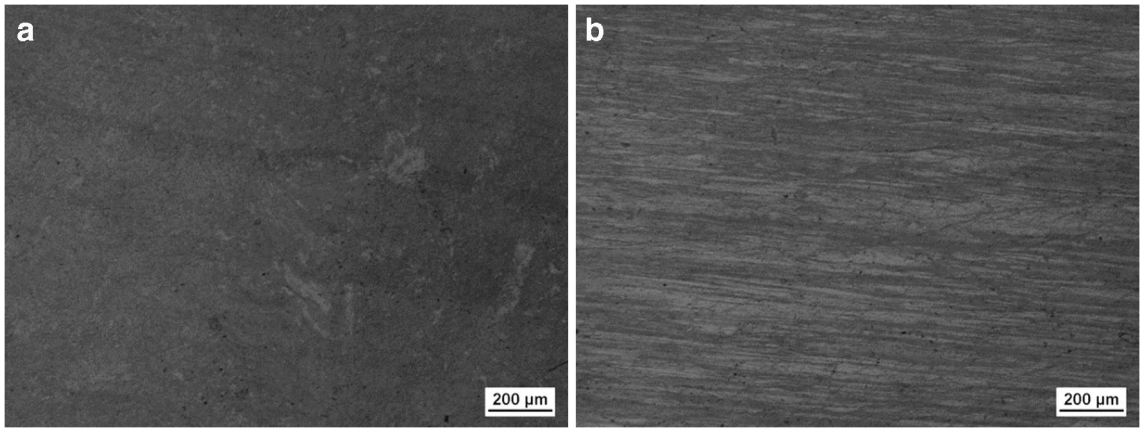

Fig. 27 Structures of Cu1Cr0.1Zr alloy in commercial temper, extruded by KOBO at 250 °C. **a** Cross-section. **b** Longitudinal section. Extrusion rate 0.5 mm/s

force, which reacts strongly to the frequency of die oscillation [39]. In turn, the process of KOBO extrusion of heat-treatable aluminum alloys eliminates their initial precipitation hardening of AA6013 [42], or as in the case of AA7075 alloy [71], "removes the effects of previous treatments." Meanwhile, the high hardness of Cu1Cr0.1Zr alloy, in commercial state, is preserved at a similar level in rods extruded by the KOBO method at low temperatures, and this parameter reacts weakly to annealing (aging).

Hardening of zinc and aluminum in the KOBO process was linked [40] to point defects with a highly non-equilibrial concentration. On the other hand, it was also acknowledged [42] that point defects could be the cause of softening of aluminum alloys, because when situated near precipitates, they relax the stresses originating from them. However, this concerns solely the case where all (nearly all) generated point defects are involved in the relaxation processes. If the number of generated point defects exceeds this value, hardening clusters strengthening the material will form during the aging process.

It can be accepted that this situation occurs in commercial Cu1Cr0.1Zr alloy extruded by the KOBO method, and this paper proves that the potential possibilities of mechanical interference in the structure of Cu1Cr0.1Zr alloy are enormous, and that its mechanical properties may be substantially higher than ever before.

5 Summary

Low-temperature KOBO extrusion of commercial Cu1Cr0.1Zr alloy, precipitation-hardened at the mill (~ 140 HV1), enables its plastic forming with a high extrusion ratio λ, and despite the elimination of the supersaturation process, makes it possible for the product to achieve a homogeneous structure, high hardening (~ 150 HV1, which corresponds to UTS ≈ 538 MPa), and specific electrical conductivity (~ 40 mS/m). Annealing (aging at 450 °C) does not affect its strength properties much in such a case; however, it does raise

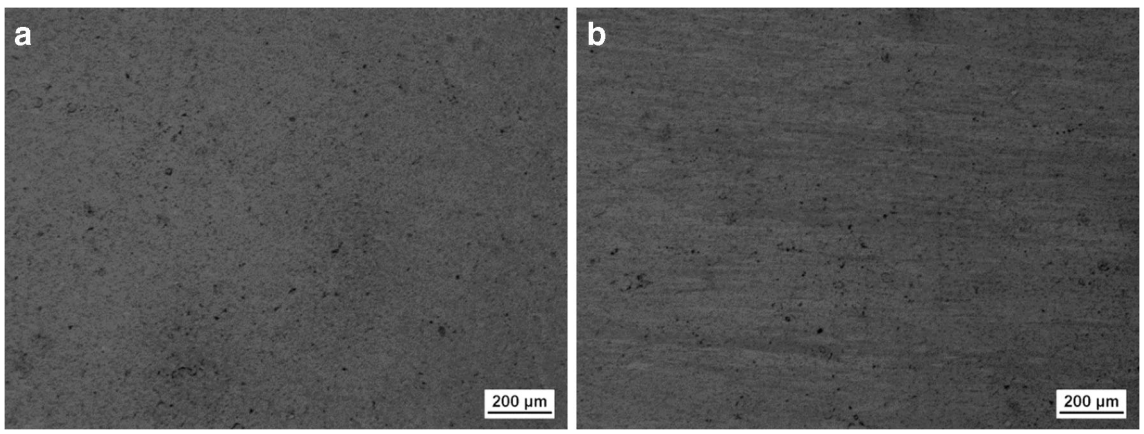

Fig. 28 Structures of Cu1Cr0.1Zr alloy in commercial temper, extruded by KOBO at 400 °C. **a** Cross-section. **b** Longitudinal section. Extrusion rate 0.5 mm/s

specific electrical conductivity. Commercial Cu1Cr0.1Zr alloy extruded by KOBO and subjected to supersaturation (950 °C/5 min or 950 °C/1 h) and aging (at 450 °C) is characterized by much lower thermal stability, although in this case also, it can reach a maximum hardness of close to 150 HV1.

Supersaturation of Cu1Cr0.1Zr alloy (900 °C/1 h) prior to the KOBO extrusion process is sufficient to harden it to a hardness of 140 HV1 (UTS ≈ 500 MPa), despite the application of temperature significantly lower than the recommended 950 °C. This is not possible in the case of supersaturation (900 °C/1 h) of alloy not deformed by KOBO, only being possible in the case of aging (450 °C/12 h). In turn, specific electrical conductivity falls drastically after supersaturation and grows successively over the course of aging at 450 °C, where the greatest changes are observed in the initial stages of this process.

In particular, the variant of KOBO extrusion of commercial CuCrZr alloy at a rate of 0.2 mm/s at temperature 250 °C should be distinguished. Despite the elimination of the annealing/aging process, the alloy is characterized by a combination of high mechanical properties (151.6 HV1) and specific electrical conductivity (43.12 mS/m).

Acknowledgments The authors are pleased to express their gratitude to Prof. L. Błaż, M.Sc. J. Lekki and M.Sc. Z. Kusion for the help in experiment. The authors are also grateful to Prof. A. Korbel for interesting discussions.

Funding information The work was supported from statutory research no. 11.11.180.960.

References

1. Zhao DM, Dong QM, Liu P, Kang BX, Huang JL, Jin ZH (2003) Structure and strength of the age hardened Cu–Ni–Si alloy. Mater Chem Phys 79(1):81–86
2. Su JH, Dong QM, Liu P, Li HJ, Kang BX (2003) Simulation of aging process of lead frame copper alloy by an artificial neural network. Trans Nonferrous Metals Soc China 13(6):1419–1423
3. Choi HL, Lee KY, Kwun SL (1997) Fabrication of high strength and high conductivity copper alloys by rod milling. J Mater Sci Lett 16(19):1600–1602
4. Zhilyaev AP, Shakhova I, Morozova A, Belyakov A, Kaibyshev R (2016) Grain refinement kinetics and strengthening mechanisms in Cu-0.3Cr-0.5Zr alloy subjected to intense plastic deformation. Mater Sci Eng A654:131–142
5. Nikolaev AK, Novikov AI, Rozenberg VM (1983) Chromium bronzes (Khromovye bronzy – in Russian). Moscow, Metallurgija
6. Chakrabarti DJ, Laughlin DE (1984) The Cr-Cu (chromium – copper) systems. Bull Alloy Phase Diagr 5(1):59–68
7. Batra IS, Dey GK, Kulkarni UD, Banerjee S (2001) Microstructure and properties of CuCrZr alloy. J Nucl Mater 299(2):91–100
8. Tang NY, Taplin DMR, Dunlop GL (1985) Precipitation and aging in high-conductivity Cu–Cr alloys with additions of zirconium and magnesium. Mater Sci Technol 1(4):270–275
9. Qi WX, Tu JP, Liu F, Yang YZ, Wang NY, Lu HM, Zhang XB, Guo SY, Liu MS (2003) Microstructure and tribological behavior of a peak aged Cu-Cr-Zr alloy. Mater Sci Eng A343(1-2):89–96
10. Zeng KJ, Hamalainen H, Lilius K (1995) Phase relatioships in Cu-rich corner of the Cu-Cr-Zr phase diagram. Scr Met Mater 32(12):2009–2014
11. Fuxiang H, Jusheng M, Honglong N, Zhiting G, Chao L, Shumei G, Xuetao Y, Tao W, Hong L, Huafen L (2003) Analysis of phases in a Cu-Cr-Zr alloy. Scr Mater 48(1):97–102
12. Holzwarth U, Stamm H (2000) The precipitation behaviour of ITER-grade Cu–Cr–Zr alloy after simulating the thermal cycle of hot isostatic pressing. J Nucl Mater 279(1):31–45
13. Amouyal Y, Divinski SV, Estrin Y, Rabkin E (2007) Short-circuit diffusion in an ultrafine-grained copper-zirconium alloy produced by equal channel angular pressing. Acta Mater 55(17):5968–5979
14. Ivanov AD, Nikolaev AK, Kalinin GM, Rodin ME (2000) Effect of heat treatments on the properties of CuCrZr alloys. J Nucl Mater 307-311(1):673–676
15. Merola M, Orsini A, Visca E, Libera S, Moreschi LF, Storai S, Panella B, Campagagnoli E, Ruscica G, Bosco C (2002) Influence of the manufacturing heat cycles on the CuCrZr properties. J Nucl Mater 307-311(1):677–680
16. Barabash VR, Kalinin GM, Fabritsiev SA, Zinkle SJ (2011) Specification of CuCrZr alloy properties after various thermomechanical treatments and design allowables including neutron irradiation effects. J Nucl Mater 417(1-3):904–907
17. Kalinin GM, Ivanov AD, Obushev AN, Rodchenkov BS, Rodin ME, Strebkov YS (2007) Ageing effect on the properties of CuCrZr alloy used for the ITER HHF components. J Nucl Mater 367-370(B):920–924
18. Zhang B, Zhang Z, Li W (2015) Mechanical properties, electrical conductivity and microstructure of CuCrZr alloys treated with thermal stretch process. Trans Nonferrous Metals Soc China 25(7):2285–2292
19. Sun LX, Tao NR, Lu K (2015) A high strength and high electrical conductivity bulk CuCrZr alloy with nanotwins. Scr Mater 99:73–76
20. Valiakhmetov OR, Galeyev RM, Salishchev GA (1990) Mechanical-properties of titanium BT8 alloy with submicrocrystalline structure. Phys Metal Metallog 10:204–206
21. Valiev RZ, Langdon TG (2006) Principles of equal-channel angular pressing as a processing tool for grain refinement. Prog Mater Sci 51(7):881–981
22. Takata N, Ohrake Y, Kita K, Kitagawa K, Tsuji N (2009) Increasing the ductility of ultrafine-grained copper alloy by introducing fine precipitates. Scr Mater 60(7):590–593
23. Vinogradov A, Patlin V, Suzuki Y, Kitagawa K, Kopytov VI (2002) Structure and properties of ultra-fine grain CuCrZr alloy produced by equal-channel angular pressing. Acta Mater 50(7):1639–1651
24. Dalla Torre FH, Pereloma EV, Daves CHJ (2006) Strain hardening behaviour and deformation kinetics of Cu deformed by equal channel angular extrusion from 1 to 16 passes. Acta Mater 54(4):1135–1146

25. Mishnev R, Shakhova I, Belyakov A, Kaibyshev R (2015) Deformation microstructures, strengthening mechanisms, and electrical conductivity in a Cu-Cr-Zr alloy. Mater Sci Eng A629:29–40
26. Valiev RZ, Islamgaliev RK, Alexandrov IV (2000) Bulk nanostructured materials from severe plastic deformation. Prog Mater Sci 45(2):45–103
27. Gertsman VY, Birringer R (1994) On the room-temperature grain growth in nanocrystalline copper. Scr Met Mater 30(5):577–581
28. Davis JW (1994) ITER Materials Properties Handbook – Technical Report. Oak Ridge National Lab, United States
29. Liang N, Liu J, Lin S, Wang Y, Wang JT, Zhao Y, Zhu Y (2018) A multiscale architectured CuCrZr alloy with high strength, electrical conductivity and thermal stability. J Alloys Compd 735:1389–1394
30. Su J, Dong Q, Liu P, Li H, Kang B (2005) Research on aging precipitation in a Cu-Cr-Zr-Mg alloy. Mater Sci Eng A392(1-2): 422–426
31. Feng H, Jiang H, Yan D, Rong L (2013) Effect of continuous extrusion on the microstructure and machanical properties of a CuCrZr alloy. Mater Sci Eng A582:219–224
32. Li YS, Tao NR, Lu K (2008) Microstructural evolution and nanostructure formation in copper during dynamic plastic deformation at cryogenic temperatures. Acta Mater 56(2):230–241
33. Han K, Walsh RP, Ishmaku A, Toplosky V, Brandao L, Embury JD (2004) High strength and high electrical conductivity bulk Cu. Philos Mag 84(34):3705–3716
34. Zhang Y, Li YS, Tao NR, Lu K (2007) High strength and high electrical conductivity in bulk nanograined Cu embedded with nanoscale twins. Appl Phys Lett 91(21):211901 1-3
35. Rozwalka J, Płaczek G, Andrzejewski D (2017) Influence of KOBO process on the properties of CuCr1Zr alloy. Metal Forming 28(2):107–122
36. Heyduk F, Ziółkiewicz S, Bochniak W, Korbel A (2015) Manufacturing rods for production of spot welding electrodes using the KOBO extrusion method. Metal Forming 26(4):325–334
37. Korbel A, Bochniak W. Method of plastic forming of materials. (1998) U.S. Patent No 5,737,959, (2000) European Patent No 0711210.
38. Bochniak W, Korbel A (2000) Plastic flow of aluminium extruded under complex conditions. Mater Sci Technol 16(6):664–669
39. Korbel A, Bochniak W, Ostachowski P, Błaż L (2011) Visco-plastic flow of metal in dynamic conditions of complex strain scheme. Metall Mater Trans A 42A(9):2881–2897
40. Korbel A, Bochniak W (2013) Lüders deformation and superplastic flow of metals extruded by KOBO method. Philos Mag 93(15): 1883–1913
41. Korbel A, Bochniak W (2017) Stratified plastic flow in metals. Int J Mech Sci 128-129:269–276
42. Korbel A, Pieła K, Ostachowski P, Łagoda M, Błaż L, Bochniak W, Pawlyta M (2018) Structural phenomena induced in course of and post low-temperature KOBO extrusion of AA6013 aluminum alloy. Mater Sci Eng A710:349–358
43. Fabritsiev SA, Zinkle SJ, Singh BN (1996) Evaluation of copper alloys for fusion reactor divertor and first wall components. J Nucl Mater 233-237(1):127–137
44. Edwards DJ, Singh BN, Toft P, Eldrup M (1998) The effect of bonding and bakeout thermal cycles on the properties of copper alloys irradiated at 100 °C. J Nucl Mater 258-263(1):978–984
45. Singh BN, Edwards DJ, Toft P (1996) Effects of neutron irradiation on mechanical properties and microstructures of dispersion and precipitation hardened copper alloys. J Nucl Mater 238(2-3):244–259
46. Edwards DJ, Singh BN, Tähtinen S (2007) Effect of heat treatments on precipitate microstructure and machanical properties of a CuCrZr alloy. J Nucl Mater 367-370(B):904–909
47. Singh BN, Edwards DJ, Tähtinen S (2004) Effect of heat treatments on precipitate microstructure and mechanical properties of CuCrZr alloy. Risø Report 1436. Risø National Laboratory, Roskilde – Denmark
48. Kalinin GM, Artyugin AS, Yvseev MV, Shushshlebin VV, Sinelnikov LP, Strebkov YS (2011) The effect of irradiation on tensile properties and fracture toughness of CuCrZr and CuCrNiSi alloys. J Nucl Mater 417(1-3):908–911
49. Korbel A, Bochniak W (1997) Economical solutions in metal forming technology. Proceedings Australasia-Pacific Forum Intelligent Processing and Manufacturing of Materials. Editors Chandra T, Leclair SR, Meech JA, Verma B, Smith M, Balachandran B. Gold Coast, 1143-1149
50. Bochniak W (2001) Mechanical properties of aluminum and AlMgSi wires produced by the KOBO mode. Aluminum: Int J Ind, Res Appl 77(6):486–489
51. Korbel A, Bochniak W, Ostachowski P, Paliborek A, Łagoda M, Brzostowicz A (2016) A new constitutive approach to large strain plastic deformation. Int J Mater Res 107(1):44–51
52. Urbańczyk-Gucwa A, Amrogowicz P, Jabłońska M, Rodak K (2016) Heat treatment of CuFe2 and CuCr0.6 alloys and the effect of precipitates on the grain refinement. Acta Phys Polon 130(A): 1016–1019
53. Hauf U, Kauffmann A, Kauffmann-Weiss S, Feilbach A, Boening M, Mueller FEH, Hinrichsen V, Heilmaier M (2017) Microstructure formation and resistivity change in CuCr during rapid solidification. Metals 7(478):1–14
54. Sauvage X, Chbihi A, Quelennec X (2010) Severe plastic deformation and phase transformations. J Phys 240(1):012003 1-8
55. Straumal BB, Pontikis V, Kilmametov AR, Mazilkin AA, Dobatkin SV, Beretzky B (2017) Competition between precipitation and dissolution in Cu-Ag alloys under high pressure torsion. Acta Mater 122:60–71
56. Straumal BB, Kilmametov AR, Korneva A, Mazilkin AA, Straumal PB, Zieba P, Beretzky B (2017) Phase transitions in Cu-based alloys under high pressure torsion. J Alloys Compd 707:20–26
57. Sauvage X, Wetscher F, Pareige P (2005) Mechanical alloying of Cu and Fe induced by severe plastic deformation of Cu-Fe composite. Acta Mater 53(7):2127–2135
58. Lojkowski W, Djahanbakhsh M, Bürkle C, Gierlotka S, Zielinski W, Fecht HJ (2001) Nanostructure formation on the surface of railway tracks. Mater Sci Eng A303(1-2):197–208
59. Mazilkin AA, Straumal BB, Rabkin E, Beretzky B, Enders S, Protasova SG, Kogtenkova OA, Valiev RZ (2006) Softening of nanostructured Al-Zn and Al-Mg alloys after sever plastic deformation. Acta Mater 54(15):3933–3939
60. Straumal BB, Kilmametov AR, Ivanisenko Y, Kurmanaeva L, Baretzky B, Kucheev YO, Zięba P, Korneva A, Molodov DA (2014) Phase transitions during high pressure torsion of Cu-Co alloys. Mater Lett 118:111–114
61. Ohsaki S, Kato S, Tsuji N, Ohkubo T, Hono K (2007) Bulk mechanical alloying of Cu-Ag and Cu/Zr two-phase microstructures by accumulative roll-bonding process. Acta Mater 55(8):2885–2895
62. Straumal BB, Kilmametov AR, López GA, López-Ferreno I, Nó ML, Sun Juan J, Hahn H, Baretzky B (2017) High-pressure torsion driven phase transformations in Cu-Al-Ni shape memory alloys. Acta Mater 125:274–285

63. Kiritani M, Satoh Y, Kizuka Y, Arakawa K, Ogasawara Y, Arai S, Shimomura Y (1999) Anomalous production of vacancy clusters and the possibility of plastic deformation of crystalline metals without dislocations. Philos Mag Lett 79(10):797–804
64. Sato K, Yoshiie T, Xu Q (2007) One dimensional motion of interstitial clusters in Ni-Au alloy. J Nucl Mater 367-370(A):382–385
65. Terentyev D, Malerba L (2004) Diffusivity of solute atoms, matrix atoms and interstitial atoms in Fe-Cr alloys: a molecular dynamics study. J Nucl Mater 329-333(B):1161–1165
66. Damsk AC, Dienes GJ (1963) Point defects in metal. Gordon and Breach Science Publishers, New York-London
67. Bakker H, Bonzel HP, Bruff CM, Dayananda MA, Gust W, Horvath J, Kaur I, Kidson GV, LeClaire AD, Mehrer H, Murch GE, Neumann G, Stolica N, Stolwijk NA (1990) Diffusion in solid metals and alloys. Springer-Verlag Berlin Heidelberg 26
68. Brandes EA, Brook GB (1992) Smithells metals reference book. Seventh Edition, Butterworth-Heinemann. Oxford, Auckland, Boston Johannesburg, Melbourne, New Delhi
69. Kawasaki M, Mendes AA, Sordi VL, Ferrante M, Langdon TG (2011) Achieving superplastic properties in a Pb-Sn eutectic alloy processed by equal-channel angular pressing. J Mater Sci 46(1): 155–160
70. Pieła K, Błaż L, Jaskowski M (2013) Effects of extrusion parameters by KoBo method on the mechanical properties and microstructure of aluminum. Arch Metall Mater 58(3):683–689
71. Korbel A, Bochniak W, Borowski J, Błaż L, Ostachowski P, Łagoda M (2015) Anomalies in precipitation hardening process of 7075 aluminum alloy extruded by KOBO method. J Mater Process Technol 216:160–168